Mycorrhiza-Triggered Transcriptomic and Metabolomic Networks Impinge on Herbivore Fitness[1]

Moritz Kaling,[a,b,2] Anna Schmidt,[c,2] Franco Moritz,[b] Maaria Rosenkranz,[a] Michael Witting,[b] Karl Kasper,[c] Dennis Janz,[c] Philippe Schmitt-Kopplin,[b] Jörg-Peter Schnitzler,[a,3] and Andrea Polle[c,3]

[a]Research Unit Environmental Simulation, Institute of Biochemical Plant Pathology, Helmholtz Zentrum München, 85764 Neuherberg, Germany
[b]Research Unit Analytical BioGeoChemistry, Helmholtz Zentrum München, 85764 Neuherberg, Germany
[c]Forest Botany and Tree Physiology, University of Goettingen, 37077 Goettingen, Germany

ORCID IDs: 0000-0002-6020-8829 (K.K.); 0000-0002-9825-867X (J.-P.S.); 0000-0001-8697-6394 (A.P.).

Symbioses between plants and mycorrhizal fungi are ubiquitous in ecosystems and strengthen the plants' defense against aboveground herbivores. Here, we studied the underlying regulatory networks and biochemical mechanisms in leaves induced by ectomycorrhizae that modify herbivore interactions. Feeding damage and oviposition by the widespread poplar leaf beetle *Chrysomela populi* were reduced on the ectomycorrhizal hybrid poplar *Populus* × *canescens*. Integration of transcriptomics, metabolomics, and volatile emission patterns via mass difference networks demonstrated changes in nitrogen allocation in the leaves of mycorrhizal poplars, down-regulation of phenolic pathways, and up-regulation of defensive systems, including protease inhibitors, chitinases, and aldoxime biosynthesis. Ectomycorrhizae had a systemic influence on jasmonate-related signaling transcripts. Our results suggest that ectomycorrhizae prime wounding responses and shift resources from constitutive phenol-based to specialized protective compounds. Consequently, symbiosis with ectomycorrhizal fungi enabled poplars to respond to leaf beetle feeding with a more effective arsenal of defense mechanisms compared with nonmycorrhizal poplars, thus demonstrating the importance of belowground plant-microbe associations in mitigating aboveground biotic stress.

Plant health and growth are influenced by complex interactions with aboveground and belowground organisms such as herbivores and mycorrhizal fungi (Pineda et al., 2013; Zeilinger et al., 2016). Mycorrhizal fungi improve nutrient acquisition and stress tolerance of their host plants (Finlay, 2008; Luo et al., 2009; Nehls et al., 2010). Mycorrhizal fungi also stimulate root proliferation (Ditengou et al., 2015) and the plant immune system, leading to induced systemic resistance (ISR; Jung et al., 2009, 2012). Thereby, the symbiosis of mycorrhizal fungi with plants modifies the interaction with aboveground herbivores (Gehring and Bennett, 2009; Hartley and Gange 2009; McCormick et al., 2014). The metabolic changes in plant leaves resulting from mycorrhizal root colonization are highly species specific (Schweiger et al., 2014). For example, plantain (*Plantago lanceolata*) colonized with *Rhizophagus intraradices* contains higher amounts of the feeding deterrents aucubin and catalpol, two bioactive iridioid (monoterpenoid) glycosides, in leaves than noncolonized plants (Gange and West, 1994). In white clover (*Trifolium repens*), mycorrhizal colonization alters the flavonoid metabolism in roots as well as in shoots (Larose et al., 2002). Colonization of tree roots with ectomycorrhizal fungi (EMF) results in decreased herbivory of the foliage (*Anomala cupripes* on *Eucalyptus urophylla* [Gange et al., 2005], *Lymantria dispar* on *Castanea dentata* [Rieske et al., 2003], and *Otiorhynchus* spp. larvae on Russian larch [*Larix sibirica*] or on *Betula pubescens* [Halldórsson et al., 2000; Oddsdottir et al., 2010]). Meta-analyses revealed divergent effects of arbuscular and ectomycorrhizal fungi on tree-insect interactions (Koricheva et al., 2009). The molecular mechanisms underlying beneficial microbe-plant interactions have mostly been studied with arbuscular

[1] This work was financially supported by the Deutsche Forschungsgemeinschaft DFG (PO361/20-2, IRGT2172 project M1, and SCHN653/5-1, 5-2).

[2] These authors contributed equally to the article.

[3] Address correspondence to jp.schnitzler@helmholtz-muenchen.de and apolle@gwdg.de.

The author responsible for distribution of materials integral to the findings presented in this article in accordance with the policy described in the Instructions for Authors (www.plantphysiol.org) is: Andrea Polle (apolle@gwdg.de).

M.K. conducted LC-MS analysis and overall data integration and wrote the draft part on metabolomics and omics data fusion; A.S. conducted the beetle and mycorrhiza experiments, provided materials, and wrote the draft section on plant performance and transcriptomics; F.M. performed mass difference network analysis; M.R. measured and analyzed VOCs and wrote the draft part on VOCs; M.W. contributed to data normalization and structural elucidations; K.K. analyzed N metabolism; D.J. analyzed the RNAseq data; P.S.-K. supervised LC-MS and mass difference network analyses; J.-P.S. designed the study, commented on data, and wrote the article; A.P. conceived the study, commented on data, and wrote the article; all authors commented and agreed on the final version of article.

www.plantphysiol.org/cgi/doi/10.1104/pp.17.01810

mycorrhizae or bacteria in herbaceous plants (Pieterse et al., 2014), whereas the systemic transcriptome-metabolome phenotypes recruited by EMF to mitigate aboveground threats to tree species are currently unknown.

Here, we investigated the impact of ectomycorrhizal colonization of poplar (*Populus* × *canescens*) roots with *Laccaria bicolor* on aboveground herbivory. Poplars are an economically relevant, fast-growing tree species planted worldwide to produce biomass and bioenergy (Polle and Douglas, 2010; Allwright et al., 2016). Infestation of poplar plantations with poplar leaf beetle (*Chrysomela populi*) can lead to great damage and economic losses (Georgi et al., 2012). Poplar leaf beetle is an abundant, specialized herbivore on poplar (Brilli et al., 2009; Müller et al., 2015). Both adult beetles and larvae prefer to feed on young leaves of the trees (Harrell et al., 1981). Whether *L. bicolor* helps its host to decrease herbivory is yet unknown, but earlier studies showed that mycorrhizal symbioses influenced leaf physiology and the levels of nutrient elements and secondary metabolites (Luo et al., 2011; Pfabel et al., 2012; Danielsen and Polle, 2014) and enhanced poplar tolerance for abiotic stress and leaf rust (Luo et al., 2009; Pfabel et al., 2012). Poplars use secondary metabolites such as phenolic glycosides, hydroxycinnamate derivatives, or condensed tannins for defense against herbivores (Tsai et al., 2006; Boeckler et al., 2011). Furthermore, benzene cyanide, aldoximes, volatiles, and antidigestive proteins (proteinase inhibitors) play a role in the defense arsenal against biotic stress (Arimura et al., 2004; Philippe and Bohlmann, 2007; Irmisch et al., 2013). However, a framework linking those diverse observations is currently lacking. Salvioli and Bonfante (2013) suggested that systems biology tools could be used to unravel complex plant-fungus interactions and the consequences for plant physiology.

In this study, we used a suite of metabolomics approaches to identify mass difference building blocks (MDBs; Moritz et al., 2017). MDBs indicate differences between metabolites (e.g. by -OH, -CH_3, or other groups) and can be interpreted as proxies for enzymatic or chemical reactions. Mass difference networks constructed with MDBs integrate all possible reactions of a certain metabolite pool and can be exploited to identify reaction types that are altered by the experimental conditions via the application of mass difference enrichment analysis (MDEA; Moritz et al., 2017). Here, we matched enriched MDBs with metabolome and transcriptome data and uncovered the biochemical pathways involved in systemic defense activation of mycorrhizal poplars. We found that *L. bicolor* inoculation reduced leaf infestation of poplar and drastically decreased the oviposition of *C. populi*. Transcriptomic and metabolomic analyses demonstrated reprogramming of defense processes in the leaves of mycorrhizal compared with nonmycorrhizal poplars. The integration of the transcriptomic and metabolomic data of leaves by network analysis revealed the down-regulation of phenolic metabolism and the induction of protease inhibitors and aldoxime biosynthesis. Thus, mycorrhizal poplars better withstood the leaf herbivore *C. populi* due to fortification with an effective arsenal of defensive mechanisms by tradeoff with constitutive phenol-based protective compounds. Because symbiotic associations between plant roots and fungi are a central component of terrestrial ecosystems, knowledge of the metabolic impact of belowground interactions on whole-plant physiology is instrumental to a functional understanding of aboveground biotic interactions.

RESULTS

Leaf Feeding and Egg Deposition of *C. populi* Are Decreased in Mycorrhizal Poplars

In this study, we grew poplars in the presence or absence of EMF in outdoor cages, in which subgroups of NC and MC poplars were exposed to poplar leaf beetles (NC = nonmycorrhizal poplars not exposed to leaf beetles, MC = mycorrhizal poplars not exposed to leaf beetles, NB = nonmycorrhizal poplars exposed to leaf beetles, and MB = mycorrhizal poplars exposed to leaf beetles; Supplemental Fig. S1). MC poplars showed 9.5% ± 0.6% mycorrhizal root tips regardless of beetle treatment ($P > 0.05$, Student's t test), whereas no EMF were observed on roots of noninoculated plants. In agreement with other studies (Colpaert et al., 1992; Langenfeld-Heyser et al., 2007; Dučić et al., 2008; Schweiger et al., 2014), EMF caused slight growth reduction in young trees (Fig. 1A, inset; Supplemental Fig. S2, A and B), probably a tradeoff between plant and fungal carbohydrate demand.

Poplar leaf beetles were given free choice between mycorrhizal and nonmycorrhizal plants. Over the time course of the experiment, significantly more beetles were present on NB than on MB poplars ($P = 0.008$, generalized linear mixed-effects model [GLM], Poisson; Fig. 1A). Consequently, feeding damage was greater on young leaves of NB compared with MB poplars ($P = 0.037$, Wilcox paired rank test), but the extent of this difference was small (Supplemental Fig. S3). Old leaves were less preferred than young leaves ($P < 0.001$, Wilcox paired rank test) and showed no differences in the foliar damage score (Supplemental Fig. S3). Because damage was confined mainly to the upper part of the plants, the loss in total leaf biomass was not excessive and ranged between 13% (MB compared with MC) and 25% (NB compared with NC; $P < 0.027$, two-sample Student's t test; Fig. 1A, inset). Beetles deposited more eggs on NB than on MB leaves ($P < 0.001$, GLM, Poisson; Fig. 1B). After 8 d of exposure during which the egg numbers increased ($P < 0.001$, GLM, Poisson), the numbers of beetles on the plants generally decreased, and more beetles were found sitting on the meshwork of the cage or on the ground. Correspondingly, leaf damage and oviposition increased only moderately after day 8 compared with the previous days (Fig. 1; Supplemental Fig. S3).

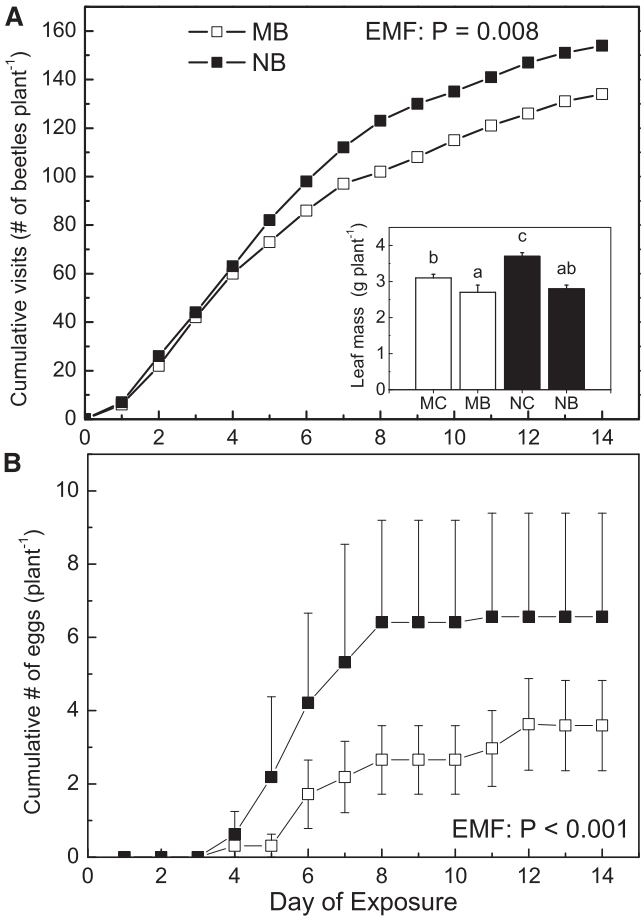

Figure 1. Visits of *C. populi*, feeding damage, and oviposition on poplar leaves of mycorrhizal or nonmycorrhizal plants. Data show cumulative visits of poplar leaf beetles and feeding damage to leaf biomass (A and inset) and cumulative number of eggs deposited on poplar leaves (B). Data indicate means ± SE ($n = 4$). Count data (beetle visits and eggs) for the whole time course were analyzed by Poisson GLM and biomass at harvest by ANOVA, with different letters denoting significantly different values.

Mycorrhizae and Leaf Herbivory Affect the Leaf Transcriptome

To decipher the molecular processes in leaves that were affected by EMF or herbivory, genome-wide transcript abundances were compared among control, EMF, and beetle treatments (Supplemental Table S1). We found a systemic response to EMF, with 146 differentially expressed genes (DEGs) in leaves under control conditions in MC compared with NC poplars (Table I, MC/NC). Among these DEGs, the Gene Ontology (GO) terms flavonoid biosynthesis, dikaempferol-4-reductase activity, response to auxin stimulus, regulation of cell development, and regulation of cell morphogenesis were specifically enriched (Table II). These results are indicative of differences in secondary metabolism and growth processes induced by EMF and, thus, underpin the phenotypic differences between MC and NC poplars (Fig. 1A, inset; Supplemental Fig. S1). Additional analyses by PANTHER revealed the highly significant GO term categories wounding response ($P < 0.001$) and response to jasmonic acid ($P < 0.0001$). These observations are important, since they suggest that EMF prepare the plants for wounding and trigger ISR, which involves jasmonate signaling (Pieterse et al., 2014).

Herbivory elicited a much stronger transcriptional response than EMF, with more than 6,000 DEGs (Table I). The overlap between the MB/MC and NB/NC treatments was considerable, with 1,902 up-regulated and 969 down-regulated DEGs (Table I). Herbivore feeding strongly affected the transcript abundance of genes in growth-, signaling-, and defense-related pathways in leaves of NB and MB plants compared with the respective controls (Table II). DEGs that responded to herbivory represented GO terms for hormone signaling, such as jasmonic acid-mediated signaling pathway, abscisic acid-mediated signaling pathway, and salicylic acid-mediated signaling pathway (Table II). Furthermore, GO terms for biotic stress were enriched, such as systemic acquired resistance (SAR), salicylic acid-mediated signaling pathway, respiratory burst involved in defense response, regulation of cell death, phytoalexin biosynthetic process, and defense response by callose deposition (Table II). Specific genes assigned to these GO terms were those encoding PR proteins, such as trypsin and protease inhibitor family proteins, monoterpene and sesquiterpene synthases (e.g. 1,8-cineole, α-humulene, and β-caryophyllene synthases), and transcription factors, especially numerous putative WRKY factors (Supplemental Table S1, count data). Transcripts with decreased abundance in leaves of beetle-challenged poplars were retrieved mainly in the GO term photosynthesis.

Since flavonoid and phytoalexin biosynthesis-related transcript abundances were altered by EMF and herbivory, DEGs were mapped to Kyoto Encyclopedia of Genes and Genomes (KEGG) pathways related to secondary metabolism and defense compounds (Supplemental Fig. S4). Almost 30% of the genes with decreased transcript abundance (21 out of 69 genes) in MC compared with NC poplars were involved in flavonoid biosynthetic processes (Supplemental Fig. S4). Unlike EMF colonization, herbivory led to increased transcript abundance of genes involved in the flavonoid pathway, regardless of whether the plants were mycorrhizal or not (NB/NC and MB/MC; Supplemental Fig. S4).

In response to herbivory, the transcript abundances of the P450 genes *CYP79D5*, *CYP79D6*, and *CYP79D7*, which are involved in the formation of aldoximes, increased independently of whether the plants were mycorrhizal or not. The herbivory-induced response was stronger in EMF than in nonmycorrhizal plants (Supplemental Fig. S5).

Mycorrhizae and Herbivory Affect the Poplar Volatile Organic Compound Pattern

The transcriptomic responses of genes encoding terpene synthases and of P450 genes involved in aldoxime biosynthesis suggested changes in the biosynthesis of

Table I. *Number of differentially expressed genes and metabolites in response to EMF inoculation and* C. populi *herbivory*

Treatment	EMF Effect			Beetle Effect		
	MC/NC	Overlap	MB/NB	NB/NC	Overlap	MB/MC
Transcriptome						
DEG up	77	2	22	2,753	1,902	2,476
DEG down	69	28	48	1,639	969	1,561
Metabolome (−)LC-MS						
Compound[a] up	12	2	42	45	99	29
Compound down	11	14	28	26	50	50
Metabolome (+)LC-MS						
Compound up	80	10	81	82	224	70
Compound down	44	12	64	148	64	94

[a]Compound is defined by the sum of the M_r values of its elements.

volatile metabolites. Therefore, we analyzed volatile organic compound (VOC) emission patterns (Supplemental Table S2). In total, 42 VOCs, including monoterpenes, sesquiterpenes, aromatic compounds, furans, and other VOCs (green leaf volatiles, fatty acids, aldehydes, and others) were detected (Supplemental Table S2). Principal component analysis (PCA) discerned the VOC profiles mainly according to the herbivore feeding (PC1, 43%; Fig. 2). However, some VOCs with minor abundance showed unique mycorrhiza-related patterns (Supplemental Table S3). For instance, the emission of 5-methyl-2-furancarboxaldehyde was suppressed in mycorrhizal poplars (NC and NB). Furthermore, MC poplars showed no detectable emission of β-ocimene, a typical herbivore-induced VOC, whereas this compound was released from NC poplars and increased upon beetle feeding in MB and NB poplars (Supplemental Table S3).

Orthogonal partial least squares discriminant analysis (OPLS-DA) revealed that 11 VOCs distinguished herbivore-exposed from nonattacked plants, among which the monoterpene β-ocimene and the sesquiterpene β-caryophyllene had the highest contributions to the model (Supplemental Fig. S6). Both terpenes are well-known herbivore-induced plant volatiles whose emissions are induced to attract parasitoids of lepidopteran species (De Moraes et al., 1998). Other herbivore-induced plant volatiles emitted by MB and NB poplars included green leaf volatiles, which are volatile products of the lipoxygenase pathway (Hatanaka, 1993), and phenolic compounds such as salicylaldehyde and phenylacetonitrile. The latter belongs to the group of phytoaldoximes, whose production was transcriptionally regulated (Supplemental Fig. S5). Phytoaldoximes are synthesized from amino acids and function either as attractants for natural enemies of herbivores or, due to their high biological activity, as direct herbivore repellents in poplar (Irmisch et al., 2013, 2014).

Mycorrhizae and Herbivory Cause Metabolic Alterations in Poplar Leaves

Poplar leaves contained a huge number of soluble metabolites, most of which have not yet been identified (Supplemental Table S4; Kaling et al., 2015). Here, we used different analytical methods, such as gas chromatography-mass spectrometry (GC-MS), ultra-performance liquid chromatography-quadrupole time of flight-mass spectrometry (UPLC-qToF-MS) in the positive and negative ion modes [(+)LC-MS and (−)LC-MS)], and Fourier transform-ion cyclotron resonance-mass spectrometry (FT-ICR-MS), for a comprehensive analysis of methanol/water-soluble leaf metabolomes and their association with chemical reactions (work flow in Supplemental Fig. S7). As the first step, PCA analyses were conducted on the compounds (defined by their molecular formulas) in the (−)LC-MS and (+) LC-MS modes. Compounds detected by (−)LC-MS clearly separated the beetle effect along PC1 as well as the mycorrhizal effect along PC2 (Fig. 3A). The separation of the beetle effect also was evident for the PCA with metabolites detected in the (+)LC-MS mode, whereas the influence of mycorrhizae was less pronounced (Fig. 3B).

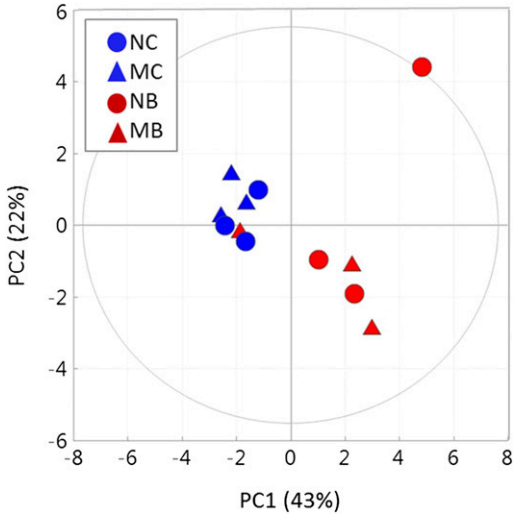

Figure 2. PCA score plot of volatile organic profiles emitted by poplar leaves. Data for the emitted volatiles are shown in Supplemental Table S3. Data were $\log_{10}$ transformed and Pareto scaled prior to analysis.

Table II. *Significantly enriched GO terms showing mycorrhizal or poplar leaf beetle effects*
n.s., Not significant.

GO Term	EMF Effect		Beetle Effect	
	MC/NC	MB/NB	NB/NC	MB/MC
Secondary metabolism				
Secondary metabolic process	<0.001	<0.001	<0.001	<0.001
Flavonoid biosynthetic process	0.005	0.013	n.s.	n.s.
Anthocyanin biosynthetic process	<0.001	<0.001	0.007	n.s.
Dihydrokaempferol 4-reductase activity	0.006	0.002	n.s.	n.s.
Phenylpropanoid biosynthetic process	<0.001	<0.001	<0.001	<0.001
Hormones				
Hormone-mediated signaling pathway	0.005	n.s.	<0.001	<0.001
Auxin metabolic process	n.s.	n.s.	0.016	<0.001
Response to auxin stimulus	0.008	n.s.	n.s.	n.s.
Jasmonic acid-mediated signaling pathway	n.s.	n.s.	<0.001	<0.001
Abscisic acid-mediated signaling pathway	0.016	n.s.	0.02	0.003
Salicylic acid-mediated signaling pathway	n.s.	n.s.	<0.001	0.018
Photosynthesis and growth				
Photosynthesis	n.s.	n.s.	<0.001	<0.001
Thylakoid	n.s.	n.s.	<0.001	<0.001
Light-harvesting complex	n.s.	n.s.	<0.001	<0.001
Regulation of cell development	0.009	n.s.	n.s.	n.s.
Regulation of cell morphogenesis/differentiation	0.025	n.s.	n.s.	n.s.
Regulation of meristem development	n.s.	n.s.	n.s.	<0.001
Cellular cell wall organization or biogenesis	n.s.	n.s.	0.016	0.007
Negative regulation of cell growth	n.s.	n.s.	0.031	0.038
Plant-type cell wall loosening	n.s.	n.s.	0.003	0.001
Lipid metabolism				
Lipid metabolic process	<0.001	n.s.	<0.001	<0.001
Lipid biosynthetic process	n.s.	n.s.	<0.001	<0.001
Fatty acid metabolic process	0.001	n.s.	<0.001	<0.001
Fatty acid biosynthetic process	n.s.	n.s.	<0.001	<0.001
Biotic stress				
Regulation of immune system process	n.s.	n.s.	<0.001	<0.001
SAR, salicylic acid-mediated signaling pathway	n.s.	n.s.	0.001	<0.001
Respiratory burst involved in defense response	n.s.	n.s.	0.041	<0.001
Plant-type hypersensitive response	n.s.	n.s.	<0.001	<0.001
Regulation of cell death	n.s.	n.s.	<0.001	<0.001
ISR	n.s.	0.046	n.s.	0.036
Phytoalexin metabolic process	n.s.	0.016	0.005	0.012
Phytoalexin biosynthetic process	n.s.	0.03	0.008	0.014
Monoterpenoid biosynthetic process	n.s.	n.s.	0.02	0.021
Toxin metabolic process	0.028	n.s.	0.007	0.001
Defense response by callose deposition	n.s.	n.s.	0.003	0.005
Defense response by cell wall thickening	n.s.	0.016	n.s.	n.s.

Discriminant analyses identified up to 167 and 86 compounds in the positive and negative ionization modes, respectively, that were up- or down-regulated in leaves of mycorrhizal compared with nonmycorrhizal control plants (Table I). Herbivory resulted in drastically higher numbers of responsive metabolites (Table I). This result illustrates that both EMF and herbivory drive the major directions of variance in the leaf metabotype (Fig. 3).

Because many compounds are still unknown, we compared the elemental composition of molecular formulas discriminant for EMF and herbivory. The majority of the compounds contained either CHO or CHNO (Supplemental Fig. S8). Of the 681 molecular equations (58%) that were discriminant for herbivory, 393 (58%) were of the CHNO type (Supplemental Fig. S8). Herbivory resulted in a higher number of down-regulated CHNO compounds in nonmycorrhizal than in mycorrhizal plants (Supplemental Fig. S8).

To obtain further information on the discriminant molecular features, they were uploaded to the MassTRIX 3 server to obtain putative metabolite annotations (Suhre and Schmitt-Kopplin, 2008). Overall, 69 (30%) and 158 (20%) molecular features were annotated for the negative and positive ionization modes, respectively. The majority of the annotated compounds belonged to the class of phenolics (Fig. 4). Both EMF and herbivory strongly affected the spectrum of phenolic compounds in leaves (Fig. 4). EMF caused the down-regulation of

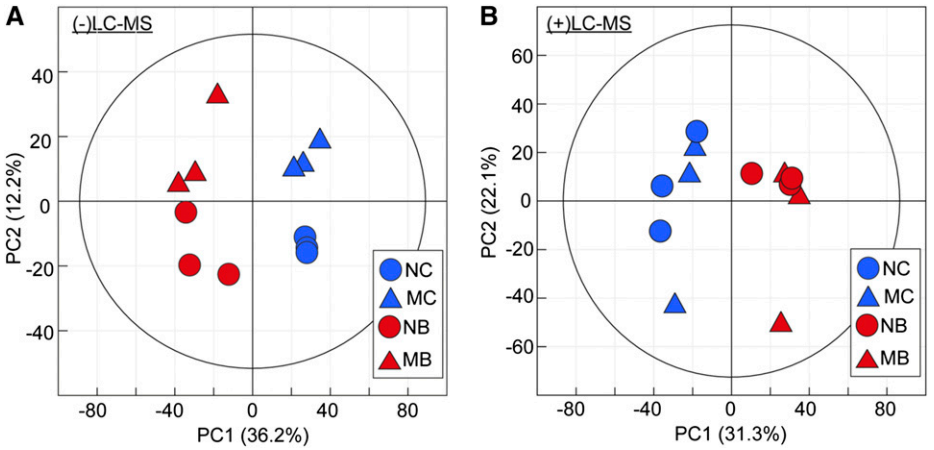

Figure 3. PCA score plot of metabolite analyses in poplar leaves for (−)LC-MS data (A) and (+)LC-MS data (B). The measurement data are shown in Supplemental Table S4.

flavonoid precursors (quercetin, dihydroquercetin, kaempferol, dihydrokaempferol, and catechine) and proanthocyanidins (two proanthocyanidin dimers and two trimers, identified by tandem mass spectrometry; Fig. 4A; Supplemental Table S4), while herbivory induced increased levels of those metabolites in both NB and MB plants (Fig. 4B). Salicinoids such as salicin-like compounds, tremulacin, populin, and salicortin-like did not respond to mycorrhization, but the latter two compounds were approximately 1.2-fold increased in response to beetle feeding in both MB and NB plants (Supplemental Table S4, negative mode of liquid chromatography-tandem mass spectrometry; refer to column heading "name"). Apparently, salicinoids were not involved in the mycorrhiza-responsive defenses.

Mapping of Transcripts onto Metabolite Data Using KEGG and MDBs

To merge transcriptomic and metabolomic data, we mapped log fold changes of metabolites and transcripts on KEGG pathways. Because EMF and herbivory both affected mainly secondary compounds, we focused our analysis on flavonoid and proanthocyanidin pathways (Fig. 5A). Metabolite and transcript abundances for

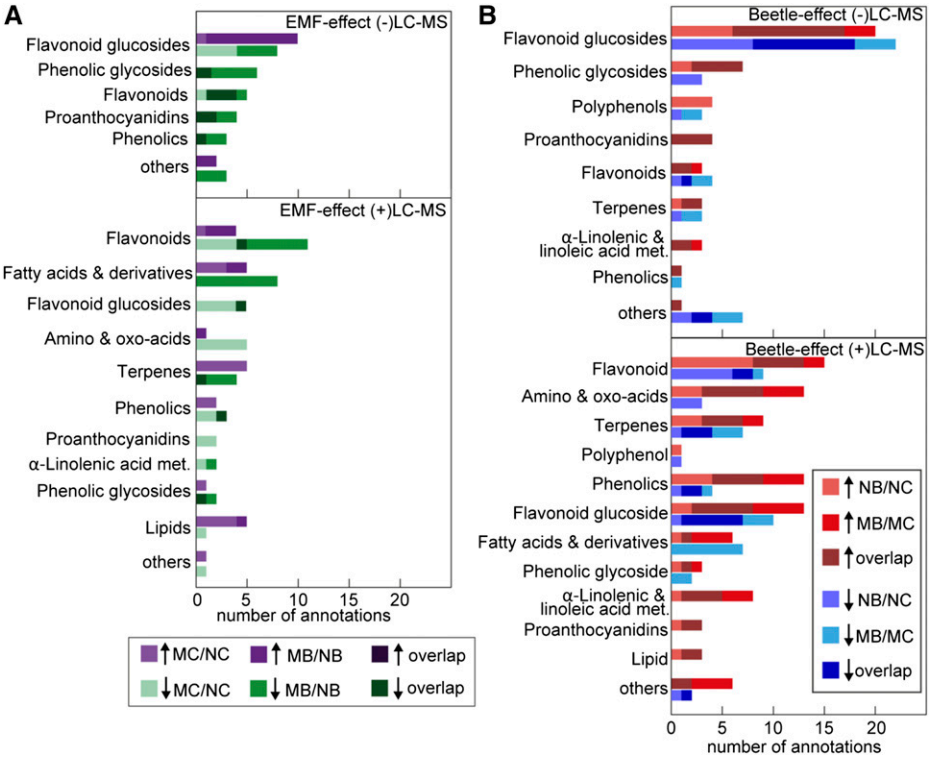

Figure 4. Numbers of compounds affected by mycorrhiza or by feeding beetles in poplar leaves. Data show numbers of annotated discriminant molecular formulas for EMF inoculation (A) and for beetle exposure (B). Bars indicate the numbers of unique or overlapping metabolites that were increased (up arrows) or decreased (doe arrows) in response to the treatment.

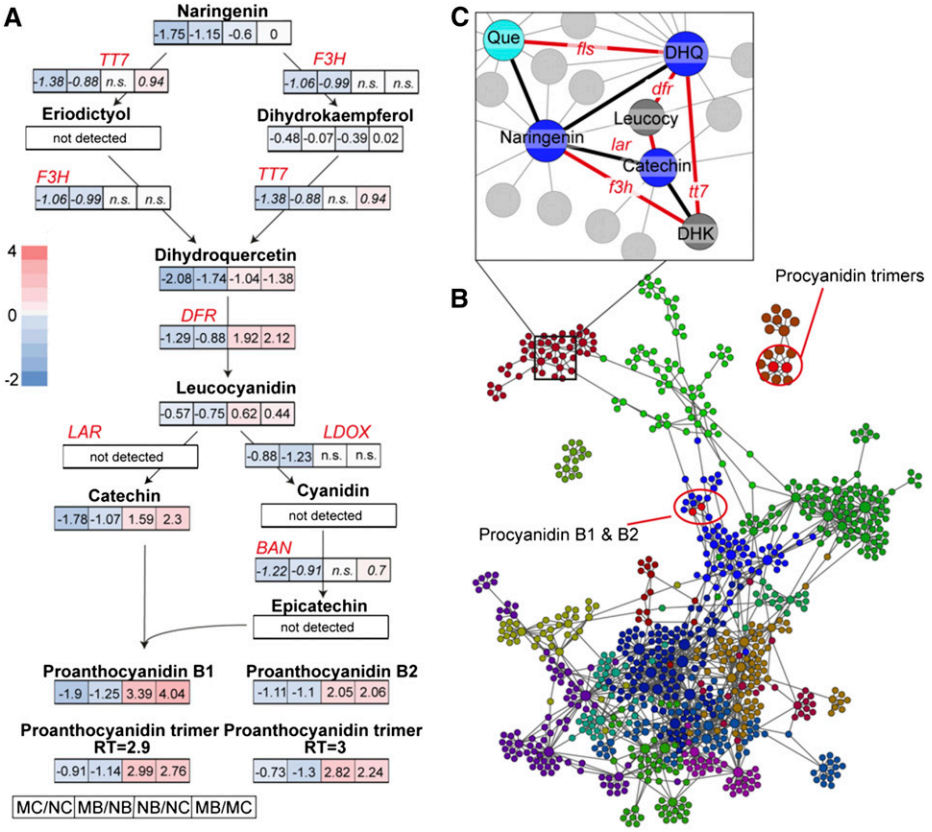

Figure 5. Flavonoid biosynthesis exemplifies transcriptomic-metabolomic data matching via MDBs. A, Log_2 fold changes of metabolite (black) and transcript (red) levels of the proanthocyanidin pathway. B and C, (−)UPLC-qToF-MS MDiN with transcripts matched on the MDBs (B; for color code of up- and down-regulated mass features, see Fig. 4) and with an expanded view of flavonoid/proanthocyanidin biosynthesis (C). Abbreviations are as follows: dihydrokaempferol (DHK), dihydroquercetin (DHQ), leucoanthocyanidin reductase (LAR), leucoanthocyanidin dioxygenase (LDOX), leucocyanidin (leucocy), quercetin (Que). The color code of the MDiN in B reflects the modularity of the nodes.

the down-regulation of flavonoid and proanthocyanidin biosynthesis under the influence of EMF and up-regulation under herbivory were closely matched (Fig. 5A). Transcript abundances of *CHALCONE SYNTHASE1*, *FLAVANONE 3-HYDROXYLASE* (*F3H*), *FLAVONOID 3′-MONOOXYGENASE* (*TT7*), *DIHYDROFLAVONOL 4-REDUCTASE* (*DFR*), *ANTHOCYANIDIN REDUCTASE* (*BAN*), and *LEUCOANTHOCYANIDIN DIOXYGENASE* were down-regulated in mycorrhizal plants and up-regulated under herbivory, corresponding to changes in metabolite levels (Fig. 5A).

To obtain further support for the chemical conversion of the flavonoid precursors, we employed mass difference network (MDiN) analysis (Moritz et al., 2017; for further explanations, see Supplemental Methodology S1). To develop the network, the MDBs, which are proxies for putative reactions, were extracted. A total of 30 MDBs were found that corresponded to reactions catalyzed by enzymes encoded by the DEGs for MC/NC (Fig. 5B). Then, all molecular formulas that were connected to at least one of the 30 MDBs were used to construct the MDiN. This resulted in an MDiN of 650 edges (representing MDBs or transcripts) and 522 nodes (metabolites). The net showed high modularity (0.76) and clustered into 14 communities (Fig. 5C). By this approach, the entire flavonoid pathway was retrieved, connecting the transcripts coding for the FLS, TT7, DFR, and LAR flavonoid pathway enzymes directly with their respective MDBs, which, in turn, were connected to their specific flavonoid educt-product pairs (Fig. 5C).

Furthermore, we found that the flavonoid monomers naringenin, dihydrokaempferol, quercetin, dihydroquercetin, leucocyanidin, and catechin clustered in a single network community (Fig. 5, B and C), while the proanthocyanidin dimers and trimers that exhibited contrasting responses to EMF and herbivory (Fig. 4) were localized in separate network communities. Flavonoids and hydrolyzable tannins, such as proanthocyanidins, are important compounds in the chemical defense of poplars against leaf herbivores (Philippe and Bohlmann, 2007). As such, it is counterintuitive that EMF induced the down-regulation of metabolite and transcript levels pertaining to a pathway that is important under herbivory. Still, the analysis of plant performance showed that *C. populi* preferred to feed and oviposit on nonmycorrhizal poplars (Fig. 1), which calls for the activation of other, more efficient defense pathways by EMF.

Induction of Aldoxime Biosynthesis Prepares Mycorrhizal Plants for Herbivore Defense

To identify putative reactions that were induced by EMF, we applied MDEA to the MDBs in the (−)LC-MS data set. Under control conditions, 13 MDBs were overrepresented in MC compared with NC poplars, among which three reactions (MDBs) pertaining to

nitrile metabolism were detected: propionitrile transfer and 2-hydroxy-2-methylbutanenitrile and hydroxymandelonitrile condensations (Fig. 6, A and B). Additionally, in MB poplars, the highest z-score was obtained for prunasin condensation (z = 3.65 of the MDB; Fig. 6B). This MDB refers to the glycosylated form of hydroxymandelonitrile, whose MDB also was overrepresented in MB/NB and MC/NC comparisons. At the same time, the condensation of Phe also was overrepresented in MB poplars. Notably, all these MDBs correspond to KEGG reaction pairs found in cyanoamino acid metabolism, where the biosynthesis of the volatile aldoxime phenylacetonitrile is located. Phenylacetonitrile was detected by GC-MS analysis, and its emission was significantly up-regulated under herbivory (Supplemental Fig. S6). Additionally, three DEGs coding for P450 monooxygenases, of which two have already been characterized to catalyze the formation of aldoxime-derived volatile nitriles (Irmisch et al., 2013), were up-regulated under herbivory (Fig. 6C; Supplemental Fig. S5). Two of those P450 enzymes, CYP79D6 and CYP79D7, possess broad substrate specificity, using at least five different amino acids as substrates (Irmisch et al., 2013). Among them is Ile, the biosynthetic precursor of 2-hydroxy-2-methylbutanenitrile, whose MDB was detected in EMF plants (Fig. 6D). Taken together, these findings substantiate the higher production of volatile nitriles as defensive compounds in leaves of mycorrhizal than nonmycorrhizal poplars.

Mycorrhizae and Herbivory Stimulate Signaling Molecules Derived from Fatty Acid Metabolism

The MDB class representing fatty acid reactions was overrepresented in leaves of mycorrhizal poplars (Fig. 6B). In the MC/NC comparison, the α-linoleic acid MDB explaining the condensation/hydrolysis of a C16 fatty acid yielded the highest z-score. Additionally, the oleolic acid condensation (C18 fatty acid) MDB was up-regulated in mycorrhizal compared with nonmycorrhizal plants (MC/NC and MB/NB). Furthermore, the MDB of the important signaling compound 9-oxononanoic acid (Wittek et al., 2014) was overrepresented in mycorrhizal and beetle-exposed (MB) poplars (Fig. 6B). This fatty acid plays an important part in SAR by priming undamaged leaves (Wittek et al., 2014).

MDEA also indicated the induction of oxidation of α-linoleic acid under herbivory independently of the mycorrhizal status (Supplemental Table S5). When plants suffer leaf damage, α-linoleic acid metabolism is induced. Enzymatic cleavage of α-linoleic acid by lipoxygenases produces C6 green leaf volatiles

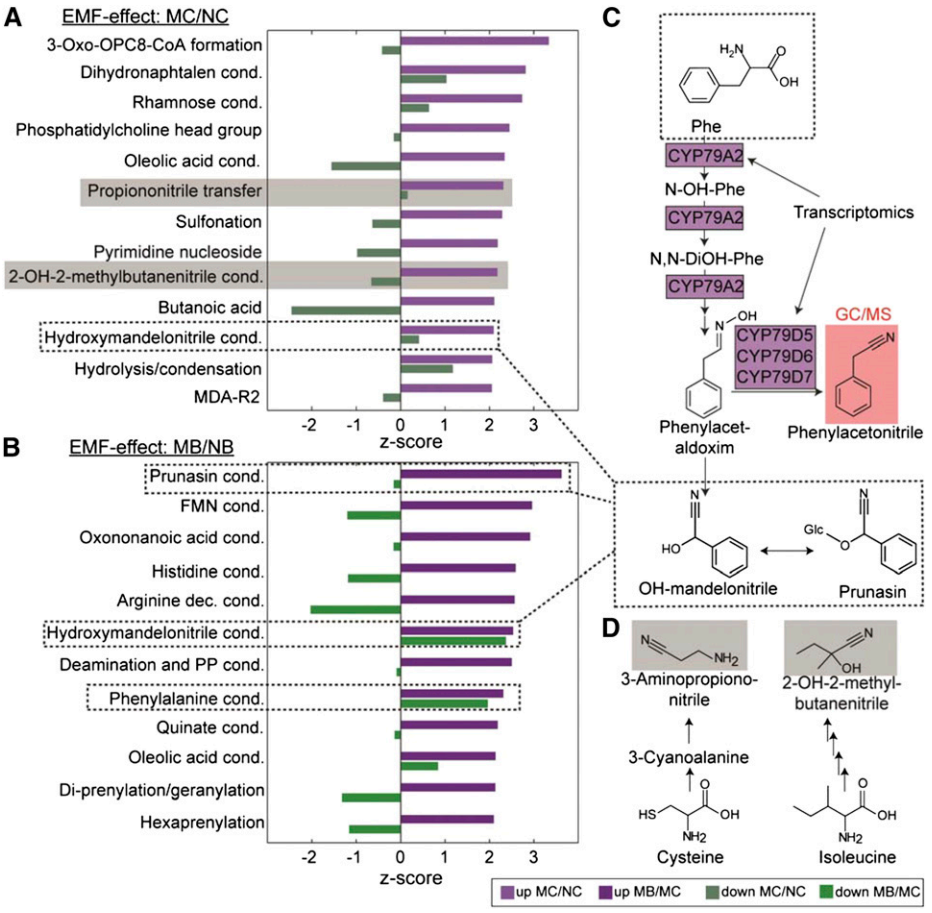

Figure 6. Z-scores obtained by MDEA of the EMF effect in the (−)LC-MS samples. A and B, Overrepresented MDBs in the MC/NC comparison (A) and the MB/NB comparison (B). C and D, MDBs highlighted with dashed lines in A and B pertain to the cyanoamino acid metabolism KEGG pathway map starting from Phe (C), and MDBs highlighted in gray start from either Cys or Ile (D). cond., Condensation; DiOH, dihydroxy; FMN, flavin mononucleotide; MDA, malondialdehyde; OH, hydroxyl. Red background, detected with GC-MS; purple background, detected via transcriptomics.

(Hatanaka, 1993; Matsui, 2006), which function as important signaling molecules, triggering defense reactions in undamaged leaves (Arimura et al., 2009). Additionally, the α-linoleic acid pathway is used for the biosynthesis of jasmonic acid and its derivatives, which are important signaling molecules in plant responses to biotic stresses (Delker et al., 2006). In agreement with the MDEA, transcriptome analyses showed enriched GO terms related to fatty acid and jasmonate metabolism for herbivory (Table II; Supplemental Table S1, count data).

MDEA also identified overrepresentation of the MDB for prenylation reactions under herbivory (Fig. 6B). In agreement with this finding, herbivory caused an induction of monoterpene and sesquiterpene emissions and enhanced levels of some higher terpenes, such as steroids, in beetle-damaged leaves. Enzymes potentially catalyzing these reactions (GDSL-like lipase/acyl hydrolases) were transcriptionally up-regulated under herbivory but also in nonstressed mycorrhizal plants (Supplemental Table S1, count data).

Cross-Platform Comparisons of Metabolites Indicate Mycorrhizal and Beetle Modulation of Nitrogen Metabolism and VOC Production

For a global view of all metabolic alterations, we applied cross-platform data matching and visualization for the four different mass spectrometric methods applied here (see "Materials and Methods") using MDiNs and MDBs. By a cross-networking approach to the mass spectrometric data, an MDiN was developed that consisted of 4,525 nodes and 114,428 edges. On this network structure, MDEA was performed for each experimental condition. Out of this MDEA, all molecular formulas discriminant for mycorrhizal plants were extracted, resulting in 68 overrepresented MDBs. These MDBs were used to display an MDiN with the responses to EMF (Fig. 7A) or herbivory (Fig. 7B). The network uncovered a treatment effect on nitrogen metabolism, because the CHNO compositional space (Supplemental Fig. S8) was up-regulated in response to mycorrhizae (Fig. 7A) but down-regulated under herbivory (Fig. 7B). To cross-check this notion, we analyzed indicators of nitrogen metabolism (Table III). EMF caused significant increases in foliar nitrogen concentrations, whereas soluble protein concentrations were unaffected by any of the treatments (Table III). MC plants displayed the highest nitrate reductase (EC 1.7.1.1) activities, and beetle exposure caused decreases in both NB and MB plants (Table III). Decreases in transcript abundances of nitrate reductase genes (*NR1* and *NR2*) also were found in NB compared with NC plants (Supplemental Table S1, count data). Since nitrate reductase is subject to post-transcriptional regulation, it is not surprising that enzyme activities did not exactly match the observed gene expression levels (Lea et al., 2006).

Furthermore, volatile compounds (Supplemental Table S3) were not distributed randomly in the MDiN but were associated directly with molecular formulas pertaining to their respective intracellular biosynthetic pathways (Fig. 7B, boxes at left). For example, sesquiterpenes were connected to farnesoic acid, the carboxylic acid of farnesyl/farnesyl pyrophosphate, which is the C15 precursor required by sesquiterpene synthases (Fig. 7B, boxes at left). Similar findings were obtained for phenylacetonitrile and salicylaldehyde, which were both connected to phenolic precursors of their respective biosynthetic pathways (Fig. 7B, boxes at left).

DISCUSSION

Systems Biology as a Tool to Uncover an Integrated Metabolic Network for an Altered Defense Phenotype

In this study, we applied modern systems biology tools to unravel the systemic effects of the ectomycorrhizal fungus *L. bicolor* on the transcriptome and chemical phenotype of poplar leaves. We used MDBs, which provide a framework for the integration of mass spectrometry-based metabolomic data into systems biology (Moritz et al., 2017; Supplemental Methodology S1). Thereby, a comprehensive MDiN was generated and analyzed by MDEA to extract the overrepresented MDBs accounting for metabolic alterations. This workflow successfully enabled us to discover important enzymatic conversions that linked the metabotype to the phenotype.

The applicability of MDiNs for cross-mass spectrometry data matching was demonstrated previously by Moritz et al. (2015) by the assignment of intracellular precursors of VOCs detected in human breath condensate. Here, MDiN-based matching of GC-MS data showed, for example, that most VOCs were in direct connection with their known cellular biosynthetic precursors, allowing for a global systemic view of metabolism. We further found that EMF-induced alterations in flavonoid biosynthesis were integrated by MDiN, because the hydroxylation and hydrolysis MDBs could be mapped onto transcripts coding for *BAN*, *F3H*, *FLS*, *DFR*, and *TT7*, which, in turn, were connected to the flavonoids quercetin, naringenin, dihydrokaempferol, dihydroquercetin, catechin, and leucocyanidin (Fig. 5). All those compounds were identified by LC-MS methods, thus validating the hypothetical reactions. These findings underpin that this novel, comprehensive approach is highly suitable to uncover systemic effects of belowground plant-fungus interactions on the aboveground plant molecular phenotype.

EMF Induce a Tradeoff of the Constitutive Phenol-Based Plant Defense

Our bioassay demonstrated that the symbiosis between *L. bicolor* and *P.* × *canescens* poplar resulted in improved poplar protection, involving decreased attractiveness of poplar leaves, slightly decreased herbivory, and reduction of beetle fitness. Our initial expectation was that EMF might have triggered an enhanced production of phenolic compounds, which constitute well-known constitutive defense mechanisms in leaves (Koricheva et al., 2009). Mycorrhizal plants often contain

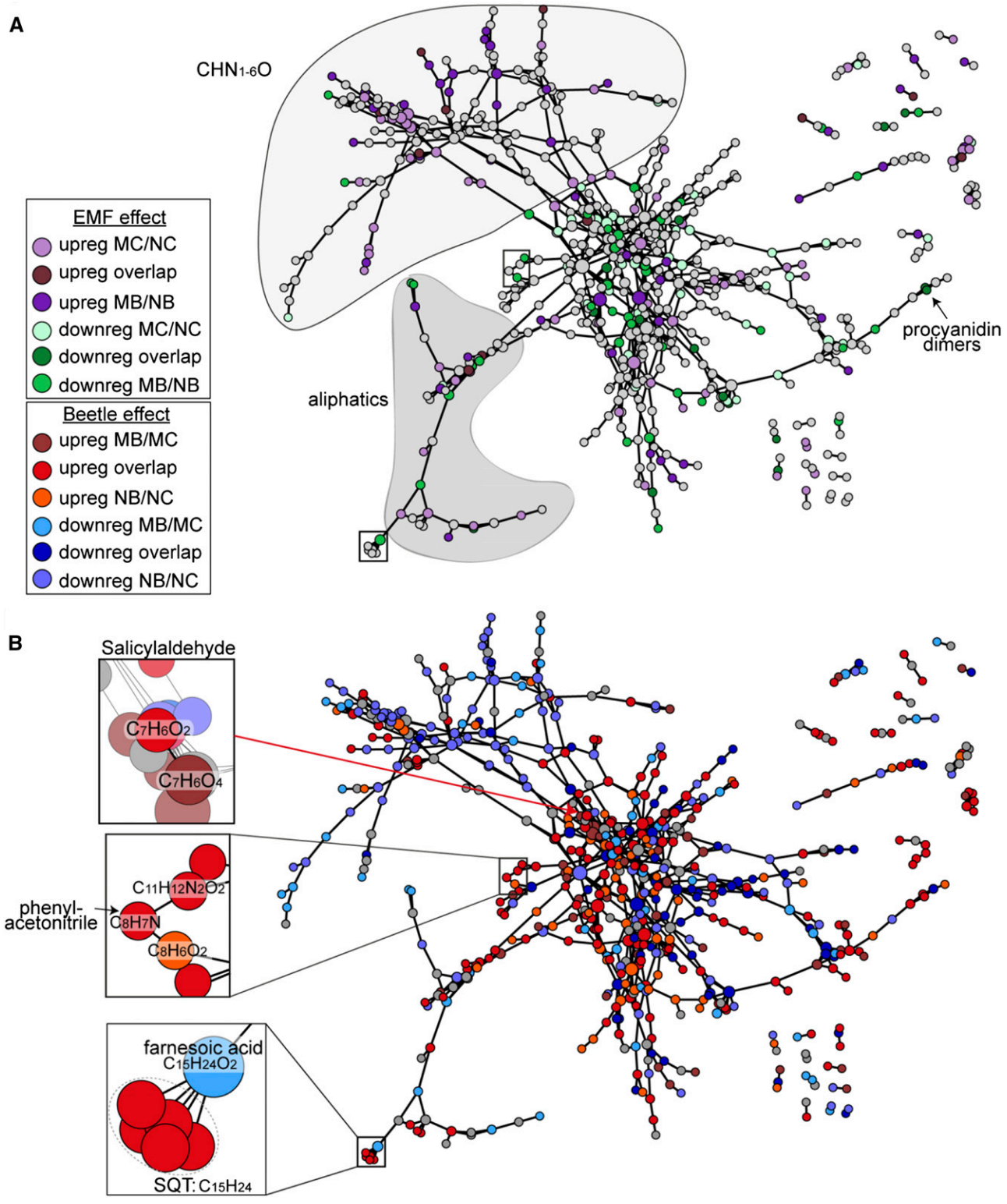

Figure 7. Cross-platform MDiN. Discriminant molecular formulas were colored according to the EMF effect (A) and according to the beetle effect (B).

Table III. *Nitrogen metabolism-related indicators*

Data show means ± SE. Different letters in rows indicate significant differences at $P < 0.05$ (ANOVA).

Parameter	NC	MC	NB	MB
Protein (mg g^{-1} dry weight)	129.9 ± 3.8 a	131.7 ± 4.5 a	143.3 ± 5.2 a	138.3 ± 3.9 a
Nitrogen (mg g^{-1} dry weight)	13.2 ± 0.2 a	15.1 ± 0.4 b	13.4 ± 0.1 a	15.1 ± 0.3 b
Carbon-nitrogen ratio	32.7 ± 0.49 b	29.1 ± 0.7 a	31.8 ± 0.4 b	29.1 ± 0.6 a
Nitrate reductase activity (μmol g^{-1} dry weight s^{-1})	2.32 ± 0.12 b	3.19 ± 0.23 c	0.64 ± 0.10 a	0.93 ± 0.33 a

higher amounts of bioactive phenolic metabolites in their leaves than nonmycorrhizal plants (Gange and West, 1994; Baum et al., 2009; Fontana et al., 2009; Schweiger et al., 2014). Moreover, phenolic compounds often are augmented under pathogen attack. For example, in hybrid poplar (*Populus trichocarpa* × *Populus deltoides*), the accumulation of tannins increased more upon rust infection in ectomycorrhizal than in nonmycorrhizal trees (Pfabel et al., 2012), but tannins are ineffective as defense compounds against a number of lepidopteran species feeding on Salicaceae species (Lindroth and St. Clair, 2013; Boeckler et al., 2014). Instead, these compounds may protect leaves against other biological hazards, and a further ecological advantage of tannin-rich leaves and insect frass is their contribution to nitrogen conservation in soil, thus benefiting tree nutrition after herbivore pressure (Madritch and Lindroth, 2015).

Poplar leaf beetles prefer to feed on young, phenolic-rich leaves (Ikonen, 2002; Behnke et al., 2010; this study). Thus, the up-regulation of transcription and metabolite levels of the flavonoid pathway upon herbivory (Fig. 4B) is unlikely to contribute to fending off poplar leaf beetle. On the contrary, chrysomelids feeding on poplar leaves can even use plant-derived secondary compounds (i.e. salicinoids after conversion to salicylaldehyde) as a bioprotectant of eggs and larvae (Rowell-Rahier and Pasteels, 1986), but this pathway was apparently not influenced by EMF.

Here, we show that EMF induced the down-regulation of tannins, flavonoids, phenolic glycosides, and proanthocyanidin dimers and trimers as well as of the transcript levels for their respective biosynthetic enzymes (Figs. 6 and 8). These decreases may render leaves less attractive because some flavonoids are feeding stimulants for chrysomelids (Matsuda and Matsuo, 1985). Changes in the biochemical composition of the leaves of EMF plants may have influenced the choice of the insects for oviposition. We suggest that the reduction in egg number on leaves of mycorrhizal poplar may result in decreased reproduction success and, consequently, could be a powerful mechanism to limit the abundance of *C. populi*, which can produce two to three generations per year (Urban, 2006).

The mechanism behind the systemic down-regulation of phenolic pathways by EMF is unknown but might indicate a tradeoff between growth, nitrogen, and defense metabolism. Ectomycorrhizae consume considerable quantities of carbon, which can amount to up to 30% of photosynthetically assimilated carbon (Rygiewicz and Anderson, 1994; Ek, 1997; Bidartondo et al., 2001). Therefore, in young mycorrhizal plants, carbon availability might have been a limiting factor for growth. The balance between growth and defense can be affected by nitrogen nutrition, although exceptions have been reported (Manninen et al., 1998; Nerg et al., 2008; Harding et al., 2009; Rubert-Nason et al., 2015; Li et al., 2016). In general, high nitrogen availability leads to a significant decrease in total phenolics (Muzika, 1993; Coviella et al., 2002; Keski-Saari and Julkunen-Tiitto, 2003; Ruan et al., 2010). In poplar leaves, tannins decrease in response to enhanced nitrogen availabilities (Madritch and Lindroth, 2015). Here, mycorrhizal plants exhibited higher nitrogen concentrations and higher levels of CHNO-containing metabolites (Table III; Supplemental Fig. S8), leading to a shift in the carbon-to-nitrogen balance, which, in turn, may have influenced phenolic compounds. Under beetle attack, nitrogen metabolism was disturbed (Table III). The decreased transcript levels for nitrate reductase (*NR1* and *NR2*) and Glu dehydrogenase and the decreased levels of nitrate reductase activities suggest a decreased provision of reduced nitrogen, which may have shifted the metabolism to increased production of phenolic compounds. Because of the links between nitrogen and secondary metabolism, we speculate that the nutritional signals caused by higher nutrient supply to mycorrhizal plants may have resulted in the observed reduction in leaf phenolic chemistry (Fig. 8). In the future, it will be interesting to investigate the nature of those long-distance signals and their potential ecological implications.

Proposed Mechanism for the Ectomycorrhizae-Induced Systemic Defense System

Beneficial microbial associations provide plants with better resistance against biotic and abiotic stresses by recruiting jasmonic acid/ethylene-dependent defense genes and abscisic acid-related pathways in distant organs in the absence of the stressor (ISR), while SAR and herbivore-induced resistance (HIR) are induced in distant, nonattacked organs by the attack of the stressor (Pieterse et al., 2014). Our experimental setup was suitable to detect components of ISR induced by EMF but not for those of HIR or SAR, since the leaves harvested from beetle-exposed plants showed symptoms of leaf feeding. EMF colonization in the absence of stress resulted in the altered expression of genes encoding orthologs of JAZ proteins (orthologs of *JASMONATE ZIM DOMAIN1* [*JAR1*] and *JAR8*) and MYB transcription factors (orthologs of *MYB4*,

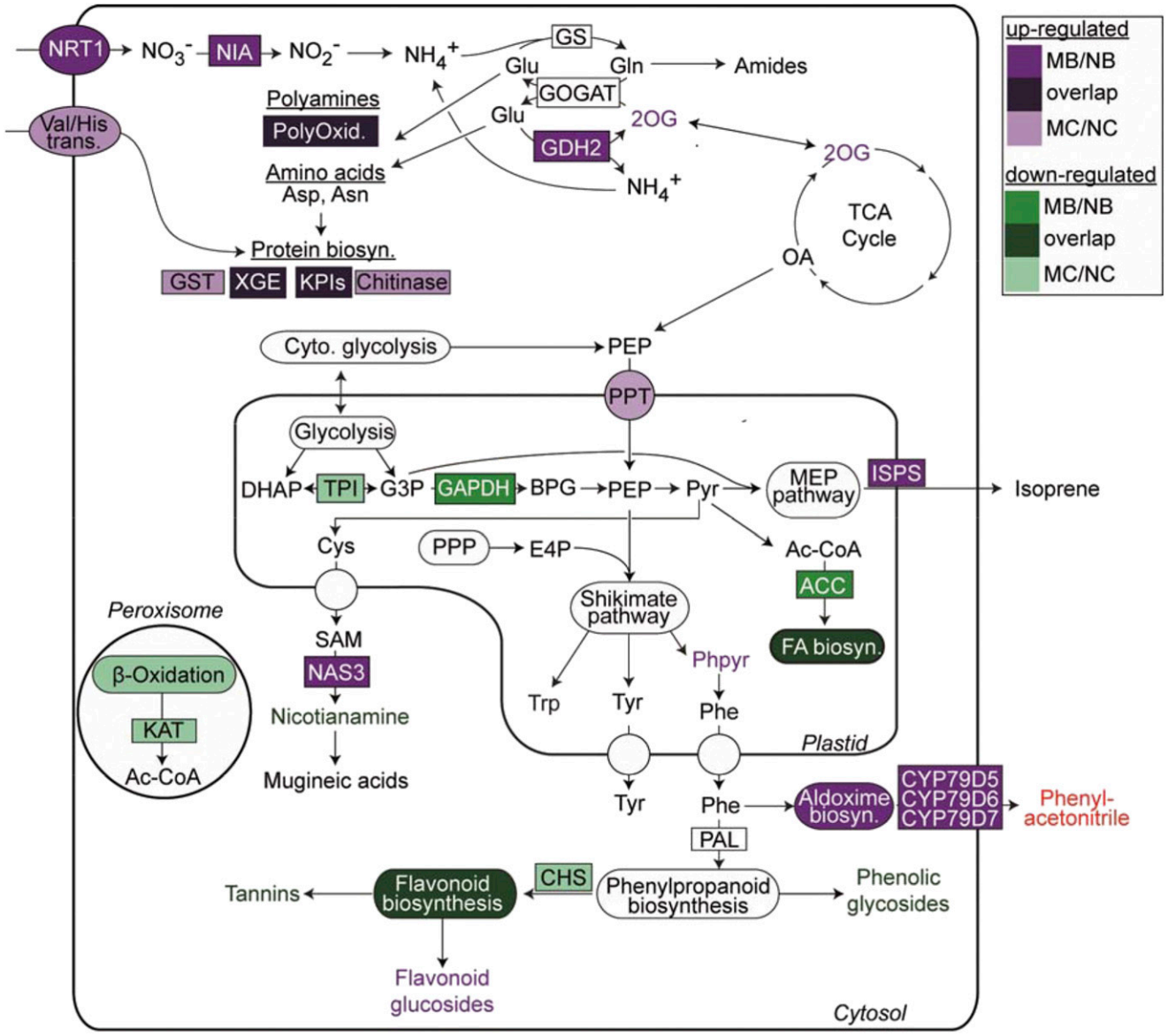

Figure 8. Illustration of systemic changes resulting from EMF inoculation within a poplar cell. Transcriptional changes of enzymes are represented by colored boxes, and those of transmembrane transporters are represented by colored circles; biosynthetic routes are illustrated in rounded rectangles that are colored according to the enzymatic and metabolic regulation patterns found within them. Metabolites and compound classes also are colored according to their respective regulation patterns. Metabolites that are colored in red were detected by GC-MS measurements. ACC, Acetyl-CoA carboxylase; Ac-CoA, acetyl-CoA; biosyn, biosynthesis; CHS, chalcone synthase; Cyto, cytosol; DHAP, dihydroxyacetone phosphate; E4P, erythrose 4-phosphate; FA, fatty acid; G3P, glyceraldehyde 3-phosphate; GAPDH, glyceraldehyde-3-phosphate dehydrogenase; GDH2, Glu dehydrogenase2; GOGAT, Gln oxoglutarate aminotransferase; GS, Glu synthase; GST, glutathione *S*-transferase; ISPS, isoprene synthase; KAT, 3-ketoacyl-CoA thiolase; KPI, Kunitz protease inhibitor; NAS3, nicotianamine synthase; NIA, nitrite reductase; NRT1, nitrate transporter; OA, oxaloacetate; 2OG, 2-oxogluterate; PAL, Phe ammonia lyase; PEP, phospho*enol*pyruvate; PPP, pentose phosphate pathway; PPT, phospho*enol*pyruvate/phosphate translocator; Phpyr, phenylpyruvate; PolyOxid, polyamine oxidase; Pyr, pyruvate; SAM, *S*-adenoysl-L-Met; TPI, triosephosphate isomerase; trans, transporter; XGE, xyloglucan endotransglucosylase.

MYB5, *MYB14*, and *MYB108*; Supplemental Table S1, count data). JAZ and MYB transcription factors are master regulators of ISR that act as negative regulators of the jasmonate/ethylene signaling pathway (Goossens et al., 2016). Induction of *JAZ* also was detected in mechanically wounded or insect-wounded poplar leaves (Major and Constabel, 2006). Suppression of the master regulators of ISR enabled the transcriptional activation of defense proteins (Goossens et al., 2016). Here, *JAZ* transcription was reduced, and wounding responses and changes in VOC patterns were elicited in the absence of stress, including an ortholog to *VEP1* (Potri.014G019700), a gene for a typical

wounding-induced enzyme that is involved in oxosteroid metabolism (Yang et al., 1997), and *GDSL-LIKE LIPASE/ACYLHYDROLASE* (Potri.004G051900; Supplemental Table S1, count data), with similarity to enzymes involved in pyrethrine production (Kikuta et al., 2011). Pyrethrines are very effective insecticides detected in members of the *Chrysanthemum* family (Matsuda, 2012). Functional characterization of the proteins encoded by Potri.014G019700 and Potri.004G051900 that may be related to pyrethrine production and their products is still required for poplar. Nevertheless, our study clearly demonstrates that EMF ameliorated plant resistance to herbivores and decreased the oviposition of the insects. We speculate that ISR might be involved in the defense response via the regulation of JAZ-related proteins, MYB factors, and the production of toxic or repellent compounds.

It was not surprising that the beetle-exposed, wounded leaves showed a massive enrichment of GO terms associated with biotic stress (Table II). The responses involved higher transcript abundances of enzymes for detoxification (glutathione *S*-transferases; Edwards et al., 2000) and nicotianamine synthase (*NAS3*) and its product nicotianamine (Fig. 8; Supplemental Table S1, count data). Nicotianamine is an important metal-chelating compound transporting Fe, Zn, and Mg (von Wiren et al., 1999; Takahashi et al., 2003; Zheng et al., 2010) and might be required for the prevention of toxic Fe oxidation products under wounding. Furthermore, we observed elevated transcript levels for genes encoding Kunitz protease inhibitors and chitinases (*KPI* and *CHI*; Fig. 8; Supplemental Table S1, count data). Protease inhibitors decrease the digestion of plant-derived proteins in the herbivore's gut (Philippe and Bohlmann, 2007). Wounding of poplar leaves results in the accumulation of chitinases (Collinge et al., 1993; Clarke et al., 1998). These enzymes hydrolyze the glycosidic bonds of chitin, the building block of an insect-derived biopolymer, and therefore function as defensive proteins. Functional analysis showed that overexpression of poplar chitinase in tomato (*Solanum lycopersicum*) inhibited the development of potato (*Solanum tuberosum*) beetles (Lawrence and Novak, 2006). Our results, therefore, indicate that poplar leaf beetle feeding induces a suite of typical defense responses.

This was also true for the VOC patterns emitted by beetle-attacked leaves. Monoterpenes, sesquiterpenes, 2-hexenal, and salicylaldehyde were among the observed VOCs (Fig. 8). These compounds are commonly emitted upon herbivory to prime other leaves' defense systems (HIR) and to attract natural herbivore enemies (Arimura et al., 2005; McCormick et al., 2012, 2014).

A highly relevant, novel result of our study was that EMF preactivated the production of important protective enzymes such chitinases and Kunitz protease inhibitors in the absence of stress. It is likely that these enzymes were recruited as the result of reprogramming hormone signaling pathways in EMF plants. In agreement with this suggestion, studies in sugarcane (*Saccharum officinarum*) showed differential regulation of chitinases in response to methyl jasmonate, abscisic acid, or salicylate exposure (Su et al., 2015). Jasmonate treatment attracted parasitoid wasps for leaf-feeding caterpillars on cabbage (*Brassica oleracea capitata*; van Dam et al., 2010). Our finding that the defense enzymes were transcriptionally less up-regulated in leaves of EMF plants upon beetle attack than in those without mycorrhizae suggests that chitinases and protease inhibitors also may act as deterrents, resulting in less feeding and, thus, lowering the requirement for defense activation.

An important result of this study was that EMF primed the aldoxime pathway. We found higher transcript abundances of genes for three P450 monooxygenases, which catalyze the formation of volatile aldoximes, in addition to enhanced phenylacetonitrile emission, during herbivory upon MB plants as compared with NB plants. These findings were supported by the MDEA results, which displayed an overrepresentation of four different nitrile MDBs pertaining to KEGG cyanoamino acid metabolism. *P.* × *canescens* is a very weak nitrile/aldoxime emitter compared with black poplar (*Populus nigra*), and upon herbivory, nitriles are generally minor components of the herbivore-induced plant VOC blend (Irmisch et al., 2013). However, nitriles and aldoximes are very effective as direct herbivore repellents and attractants of natural enemies of herbivores (Irmisch et al., 2013, 2014; McCormick et al., 2014). In our study, the attraction of predators was excluded, but the enhanced aldoxime production in leaves of mycorrhizal plants may have contributed to the preference of leaf beetles for nonmycorrhizal plants.

In summary, the interaction of poplar roots with the ectomycorrhizal fungus *L. bicolor* resulted in the systemic adjustment of defense mechanisms in leaves, consisting of transcriptional and metabolic enhancement of protease inhibitors, chitinases, volatiles, aldoximes, and nitrogen-bearing compounds, while phenolics were decreased in the foliage. These alterations influenced the choice of poplar leaf beetles for oviposition. We speculate that enhanced nitrogen allocation to leaves enabled mycorrhizal poplars to increase the production of protease inhibitors and volatile nitriles and to lower the production of plant phenolics in leaves for a more effective control of specialist herbivores such as *C. populi*. By employing a systems biology approach, we demonstrated that mycorrhizae can reprogram the defense system from constitutive to specialized defenses. Our study revealed that belowground interactions, which are ubiquitous in ecosystems, change the plant metabolism drastically, directly influencing aboveground plant-insect interactions. Future studies must be aware of these effects and should include them in their data evaluation.

MATERIALS AND METHODS

Plant Material and Inoculation of Poplar with the Mycorrhizal Fungus *Laccaria bicolor*

The ectomycorrhizal fungus *L. bicolor* (strain S238N-H82) was cultivated for 3 weeks in a sandwich system on a sand/peat mixture (two parts peat [REWE], eight parts coarse sand [diameter: 0.71–1.25 mm; Melo], and two parts fine sand

[diameter: 0.4–0.8 mm; Melo]) as described by Müller et al. (2013). For the controls, a sand/peat mixture without adding the fungus was prepared in the same way.

Before planting, the sand/peat mixture with or without fungus was mixed with 3 L of the same sand/peat mixture, as described by Müller et al. (2013). Gray poplar (*Populus* × *canescens*, syn. *Populus tremula* × *Populus alba*; INRA clone 717-1B4) was grown under axenic conditions for 2 weeks on rooting medium and planted directly in the sand/peat mixture in 3-L pots, either with or without fungal inoculum, and gradually acclimated to greenhouse conditions of 17.9°C ± 0.5°C and 68.7% ± 2.4% air humidity as described by Müller et al. (2013). The poplars were automatically irrigated three times daily with 10 mL for the first 5 weeks and thereafter with 20 mL using an irrigation system with a Long Ashton solution as described by Müller et al. (2013).

Three weeks before the beetle bioassay, the plants were placed in eight cages (190 cm × 140 cm × 190 cm) covered with mesh screen (mesh size, 1.4 mm; thickness, 0.28 mm; Supplemental Fig. S1A). Each cage contained eight *L. bicolor*-inoculated (M) and eight noninoculated (N) poplars (Supplemental Fig. S1B). Four cages were designated as controls (MC and NC) and four as beetle treatments (MB and NB). The height of each plant was measured biweekly until the end of the experiment.

Exposure of Poplar to *C. populi* Beetles

Ten weeks after the EMF inoculation, the NB and MB poplars were exposed to *C. populi*. Adult beetles were collected in a 5-ha-large, 4-year-old commercial poplar plantation (Max4 and Monviso [*Populus maximowizcii* × *Populus nigra* and *Populus* × *generosa* × *P. nigra*]) in southern Germany (Díaz-Pines et al., 2016). Since mycorrhizae establish on poplars within the first year after planting (Danielsen et al., 2013), we assumed that the trees were mycorrhizal. A total of 320 beetles were released in four cages (80 beetles per cage) by placing 10 insects between each pair of the mycorrhizal and nonmycorrhizal plants. For the following 14 d, the beetles had free choice between NB and MB plants. The localizations of the beetles and the egg depositions were recorded every day. To investigate the feeding behavior of the beetles, a ranking scale for the fed leaf area of each single leaf was used. The visual scale range was 0 (undamaged), 1 (less than 10% fed), 2 (10%–25% fed), 3 (25%–50% fed), 4 (50%–75% fed), and 5 (more than 75% fed; Supplemental Fig. S3).

Sampling and Analysis of VOCs

VOCs were collected in the headspace from the top six feeding-damaged poplar leaves enclosed in a polytetrafluoroethylene bag (Toppits; 25 cm × 40 cm, volume of 2.5 L; $n = 3$ per treatment). The same setup without poplar enclosure was sampled as the background control. The VOCs were collected for 1.5 h by headspace sorptive extraction (HSE) using the stir bar sorptive extraction method with Gerstel Twisters (Gerstel). The twisters were attached to the tops of long magnetic sticks placed in the pots and enclosed in the polytetrafluoroethylene bags together with the six topmost leaves. Sensitivity changes during sample analysis were taken into account by adding δ-2-carene as an internal standard onto the twisters.

The samples were analyzed with a thermodesorption unit (Gerstel) coupled to a gas chromatograph-mass spectrometer (gas chromatograph model, 7890A; mass spectrometer model, 5975C; Agilent Technologies) as described by Weikl et al. (2016). The chromatograms were analyzed by the enhanced ChemStation software (MSD ChemStation E.02.01.1177; Agilent Technologies). The poplar VOCs reported by Irmisch et al. (2013) and Müller et al. (2015) were screened manually in the total ion currents (TIC). The identification of VOCs was achieved by comparing the obtained mass spectra with those of authentic standards that are commercially available (Sigma-Aldrich) or with NIST 05 and Wiley library spectra. The TIC of each VOC in the final data set was recalculated from the absolute abundance of the first representative mass-to-charge ratio (m/z) to eliminate noise. Quantification of the compound concentrations was conducted using the TIC of external standards: isoprene and α-pinene for nonoxygenated monoterpenes, linalool for oxygenated monoterpenes, (E)-caryophyllene for nonoxygenated sesquiterpenes, nerolidol for oxygenated sesquiterpenes, and toluene for other VOCs. The representative m/z and retention indices of the remaining VOCs were calculated according to van den Dool and Kratz (1962). Emission rates (pmol m^{-2}) were calculated based on enclosed leaf area and exposure time of the twisters. Compared with dynamic VOC sampling in continuously flushed cuvettes (Tholl et al., 2006), passive sampling of VOCs by HSE in closed bags results in semiquantitative rather than absolute data for the emission rate. Nevertheless, changes in emission pattern and relative treatment effects, similar to the metabolomic data set, can be analyzed.

For statistical analysis, the VOC concentrations were utilized as variable X for OPLS-DA analysis. The X variables were Pareto scaled, and the four experimental parameters (MC/NC, MB/NB, MB/MC, and NB/NC) were assigned as Y variables. Unfortunately, partial least squares and OPLS-DA models explaining the mycorrhizal (MB/NB and MC/NC) and beetle (NB/NC and MB/MC) effects separately had negative Q^2 (second quantile) values. Therefore, the beetle treatments (NB and MB; $n = 6$) were tested against nonexposed treatments (MC and NC; $n = 6$). Discriminant volatiles were extracted from the S plot, which was constructed from the OPLS-DA model, based on their correlation value [$P_{(corr)} > 0.8$].

Harvest of Plant Material and Biometric Analyses

From each plant, leaf 5 from the stem apex was harvested 8 d after release of the beetles. The leaves in the beetle-exposed cages showed feeding symptoms. Leaf samples for each treatment and cage were pooled, resulting in four biological replicates per treatment. Leaves were immediately frozen in liquid nitrogen and stored at −80°C.

After 14 d of beetle exposure, all plants were harvested. Fresh masses of stems and leaves were recorded. Two fresh leaves of each plant were weighed and scanned to calculate the total leaf area. To determine dry weight, the plant materials were dried at 60°C for 7 d. The root system was washed, separated into fine (less than 2 mm in diameter) and coarse roots, and weighed. Root samples were kept at 4°C in plastic bags for further analysis. Randomly selected subsamples of the roots were examined with a stereomicroscope (DFC 420 C; Leica). To calculate the EMF colonization rate, the numbers of mycorrhizal, nonmycorrhizal, vital, and nonvital root tips were counted for 200 root tips per plant. The EMF colonization rate was calculated as follows: number of mycorrhizal root tips/(number of mycorrhizal root tips + number of nonmycorrhizal vital root tips). After root analysis, the dry weight of the roots was determined.

Statistical analyses of plant and beetle performance were done using R (http://www.r-project.org/). The normal distribution of data was tested with the R function shapiro.test (https://stat.ethz.ch/R-manual/R-devel/library/stats/html/shapiro.test.html; R Core Team 2015). Count data for locations of beetles and eggs were compared by fitting a Poisson GLM using the R function glmer from the lme4 package (Bates et al., 2015), specifying the treatment level (mycorrhized/nonmycorhized) as a fixed effect and allowing for the different cages as a random effect. The effect of mycorrhization on feeding damage was compared by first calculating the mean values of all leaves of one treatment group per day and cage and subsequently applying a paired Wilcoxon rank sum test (treatment paired over day and cage number) using the R function wilcox.test from the stats package (https://stat.ethz.ch/R-manual/R-devel/library/stats/html/wilcox.test.html). Normally distributed data (plant height and biomass) were subjected to ANOVA followed by a posthoc Tukey's test (Hothorn et al., 2008; http://multcomp.r-forge.r-project.org). Means were considered to indicate significant differences at $P \leq 0.05$.

Protein, Nitrate Reductase, Nitrogen, and Carbon Determination

Top leaf 7 or 8 from the apex was extracted in extraction buffer (50 mM Tris-HCl [pH 8], 3 mM Na_2-EDTA, 0.5 (v/v)% Triton, and 100 mg mL^{-1} insoluble polyvinylpolypyrrolidone; Polle et al., 1990). Extracts were used for soluble protein determination with Coomassie reagent (Coomassie Plus [product 23236]; Thermo Scientific) and for spectrophotometric determination of nitrate reductase activity after Schopfer (1989). The test was calibrated with $NaNO_2$.

For carbon and nitrogen analyses, leaves were dried, milled, and weighed into tin cartouches. The samples were analyzed in Elemental Analyzer EA1108 (Carlo Erba Strumentazione). Acetanilide (71.09 (w/w)% C and 10.36 (w/w)% N; Carlo Erba Strumentazione) was used as the standard.

Data were distributed normally and, thus, tested by ANOVA followed by a posthoc Tukey's test as described above.

RNA Sequencing, Transcript Analyses, and Reverse Transcription-Quantitative PCR

Total RNA was extracted from the biological replicates of the NC, MC, NB, and MB treatments. The leaves were ground in liquid nitrogen in a ball mill

(Retsch), and 500 mg of powder was used for RNA extraction according to the method described by Chang et al. (1993).

RNA quality was checked using a Bioanalyzer (Agilent 2100; Agilent). The RNA integrity numbers ranged from 6 to 6.4. Library construction and sequencing were conducted at Chronix Biomedical. RNA libraries were prepared using the Mint-2 Kit (Evrogen). Single-end reads were sequenced with a length of 100 bp in two lanes on an Illumina HiSeq 2000. In each lane, six samples were sequenced. Before processing, each sample consisted of ~31 to 39 million reads. Processing of the raw sequence data was performed with the FASTX toolkit (http://hannonlab.cshl.edu/fastx_toolkit/). Using FASTQ Trimmer, all nucleotides with a Phred quality score below 20 were removed from the ends of the reads, and sequences smaller than 50 bp or sequences with a Phred score below 20 for 10% of the nucleotides were discarded (http://hannonlab.cshl.edu/fastx_toolkit/). Adapter sequences and primers were removed with FASTQ Clipper (http://hannonlab.cshl.edu/fastx_toolkit/). After processing, ~25 to 32 million reads per sample remained. The reads are permanently stored in the European Nucleotide Archive under accession number PRJEB21029.

The processed sequences were mapped against the *Populus trichocarpa* transcriptome (downloaded from http://phytozome.net) using Bowtie (http://bowtie-bio.sourceforge.net). Furthermore, using Bowtie, count tables of transcripts were generated. Transcripts were assigned to *P. trichocarpa* identifiers and annotated to homologous Arabidopsis (*Arabidopsis thaliana*) gene identifiers (Arabidopsis Genome Initiative identifiers; Tsai et al., 2011; http://aspendb.uga.edu/downloads). To find transcripts with significantly increased or decreased abundance, the edgeR package (Robinson et al., 2010; http://www.bioconductor.org/packages/release/bioc/html/edgeR.html), implemented in R (http://www.r-project.org/), was used. To estimate overrepresented GO terms, an enrichment analysis was performed with The Ontologizer software (Bauer et al., 2008; http://www.geneontology.org/). Overrepresented GO terms at $P < 0.05$ were determined by parent-child union with Benjamini-Hochberg correction (Benjamini and Hochberg, 1995). In addition, the best Arabidopsis Genome Initiative matches were uploaded in PANTHER (release of April 13, 2017; http://go.pantherdb.org/) and analyzed by GO Slim terms. To visualize pathways, transcriptomic data were uploaded in the software Paintomics (version 2.0; http://www.paintomics.org).

To validate RNA sequencing (RNAseq) count data, three genes (*NITRITE REDUCTASE1* [*NIR1*], *JASMONATE ZIM DOMAIN-LIKE10* [*JAZ10*], and *GLN SYNTHASE2* [*GS2*]) were selected that covered a range from low to high count data in the RNAseq data set and showed significant changes among treatments (*NIR1* and *JAZ10*) or not (*GS2*). Primers were designed for *P.* × *canescens* (Supplemental Table S1, validation), and reverse transcription-quantitative PCR analyses were conducted as described previously with *ACTIN* as the reference gene (Kavka and Polle, 2016). Relative transcript abundance was expressed as $E^{(\text{ct of } actin)}/E^{(\text{ct of test gene})}$ with E = primer efficiency. Relative transcript abundances were fitted against RNAseq count data and revealed a highly significant linear correlation (Supplemental Table S1, validation).

Metabolite Extraction

Fifty milligrams of powdered leaf material was extracted twice with 1 mL of −20°C methanol:water (8:2 [v/v]) at 0°C for 15 min. Subsequently, the solution was centrifuged at 10,000*g* for 10 min at 4°C. A total of 1.5 mL of supernatant was divided into two aliquots of 750 μL. For quality control, 20 μL of each extract were taken and combined. One aliquot was used for direct injection FT-ICR-MS measurements. From the second aliquot, the extraction solvent was removed in a Speed-Vac and stored at −80°C for further analysis. Prior to the UPLC-qToF-MS measurements (see below), the dried samples were resolved in 500 μL of 20% (v/v) acetonitrile in water and centrifuged at 19,500*g* at 4°C for 10 min.

FT-ICR-MS Measurements and Data Analysis

Ultra-high-resolution mass spectra were acquired using an FT-ICR-MS device (APEX Qe; Bruker) as described by Kaling et al. (2015). Measurements were performed in the negative ionization mode over a mass range of *m/z* 100 to 1,000. The resulting mass spectra were internally calibrated and exported to peak height lists at a signal-to-noise ratio of 2 using the Data Analysis 4.0 software package (Bruker). The peak lists were combined to a peak matrix with an error of 1.5 ppm using an in-house written tool (Lucio et al., 2011). Peaks with just one nonzero intensity (single mass events) were removed from the matrix as well as peaks that were detected in less than 50% of all biological replicates. After that, a ^{13}C isotopic peak filter was applied, deleting peaks with no corresponding ^{13}C isotopic peak to avoid signals generated by electrical noise. Intensities were total ion current (TIC; sum of all intensities) normalized (Intensity/TIC)*TIC(average) and used for statistical analysis.

For molecular formula annotation of the unknown *m/z* features, the filtered mass list was subjected to the mass difference-based NetCalc algorithm of Tziotis et al. (2011). The NetCalc annotation procedure was repeated 10 times. Molecular formulas that were annotated in each individual run were used for LC-MS matching.

UPLC-qToF-MS Measurements and Data Analysis

LC-MS measurements were performed on the Waters Acquity UPLC System (Waters) coupled to the Bruker maXis ToF-MS (Bruker Daltonic). Chromatographic separation was achieved on a Grace Vision HT C18-HL column (150 mm × 2 mm i.d. with 1.5-μm particles; W.R. Grace). Eluent A was 5% acetonitrile in water with 0.1% formic acid, and eluent B was acetonitrile with 0.1% formic acid. The gradient elution started with an initial isocratic hold of 0.5% B for 1 min, followed by a linear increase to 99.5% B in 5.4 min, and a further isocratic step of 99.5% B for 3.6 min. In 0.5 min, the initial conditions of 0.5% B were restored. To equilibrate the initial column conditions, 0.5% B was held for 5 min. The flow rate was 400 μL min^{-1}, and the column temperature was set at 40°C. The autosampler was set to 4°C. From each sample, two technical replicates were measured in both the positive and negative ionization modes. Mass calibration was achieved with low-concentration ESI Tuning Mix (Agilent).

The mass spectrometer was operated as follows: nebulizer pressure was set to 2 bar, dry gas flow was 8 L min^{-1}, dry gas temperature was 200°C, capillary voltage was set to 4,000 V, and the end plate offset was −500 V. Mass spectra were acquired in a mass range of 50 to 1,100 *m/z*.

The LC-MS spectra were internally calibrated with the ESI Tuning Mix. Each Bruker spectrum file was imported separately into the GeneData Refiner MS software (Gendata). After chemical noise reduction and retention time (RT) alignment, the *m/z* features were identified using the summed-peak-detection feature implemented in the GeneData software. Only peaks that were present in at least 10% of mass spectra were used for isotope clustering. The resulting peak matrix was exported and used for further processing steps.

To adjust for technical variations, cyclic loess normalization was applied (Ejigu et al., 2013) using the R packages Bioconductor (http://www.bioconductor.org/) and Library(affy). Two normalization cycles (x = 2) were needed to eliminate batch effects of the negative mass spectra, and one cycle (x = 1) was needed to eliminate the batch effect of the positive measurements. After that, the average peak intensity of both technical replicates was calculated. If a peak was detected in only one technical replicate, it was removed from the matrix.

The molecular formula/intensity matrices were imported into SIMCA-P (version 13.0.0.0; Umetrics) for multivariate statistical analysis. Discriminant molecular formulas were determined by OPLS-DA. For each experimental condition (MC/NC, MB/NB, NB/NC, and MB/MC), separate OPLS-DA models were calculated, in which either mycorrhizae or beetles were Y variables [e.g. for mycorrhiza: Y(inoculated) = 1 and Y(noninoculated) = 0]. Molecular formulas with a variable influence of projection score > 1 and an acceptable cross-validation SE were extracted. When these features possessed a $\log_2$ fold change > 1 or < −1, they were considered as discriminant.

MDEA of LC-MS Data and Mapping on Transcriptomic Data

It was shown recently (Forcisi et al., 2015) that the network-based molecular formula assignment of Tziotis et al. (2011), which is usually used on high-resolution MS instruments, also is applicable to mass spectra with lower resolution. Furthermore, Moritz et al. (2017) demonstrated how MS data can be used to link metabolomes to genotypes via MDBs. Based on these techniques, we developed a workflow that mapped the results obtained by mass difference analysis onto the transcriptomic data. A scheme of the data analytical workflow is given in Supplemental Figure S7.

In a first step, the filtered FT-ICR-MS *m/z* list was subjected to mass difference network-based molecular formula annotation (NetCalc) using an MDB list consisting of 450 reactions (Moritz et al., 2017). This procedure clustered the compounds according to mass differences and predicted chemical reactions that converted educts into products (Moritz et al., 2017). This procedure resulted in the assignment of 2,789 molecular formulas. To achieve cross-omics data integration by means of MDB transcript matching, all transcripts coding for metabolic enzymes were assigned to their respective EC numbers. Then, the EC numbers were matched on their respective KEGG reaction pairs (Moritz et al., 2017), which were then mapped to the MDBs (Supplemental Fig. S7).

In the next step, the low-resolution (−)LC-MS data were annotated following the procedure described by Forcisi et al. (2015). To further improve the accuracy of these annotations, they were matched with the FT-ICR-MS annotations. The 432 molecular formulas (without isomers) that were assigned in both the (−) LC-MS and (−)FT-ICR-MS measurements were used as new starting masses for a follow-up round of 100 consecutive (−)LC-MS annotation runs. Finally, 2,422 stable molecular formulas were used to reconstruct a theoretical (−)LC-MS MDiN.

To annotate (+)LC-MS *m/z* features, molecular formulas possessing an annotation frequency greater than 90% were used for the creation of mass-difference retention time rules (Forcisi et al., 2015). The resulting retention time mass differences were used for a second round of 100 NetCalc annotations, deleting incorrect molecular formula annotations. At the end, 2,644 molecular formulas could be used for the reconstruction of the theoretical (+)LC-MS MDiN.

Accession Number

Short reads are stored in the European Nucleotide Archive under accession number PRJEB21029.

Supplemental Data

The following supplemental materials are available.

Supplemental Figure S1. Setup of the *C. populi* exposure experiment with mycorrhizal or nonmycorrhizal *P.* × *canescens* under outdoor conditions.

Supplemental Figure S2. Height increment before and after herbivory and biomass of mycorrhizal and nonmycorrhizal poplars in the absence or presence of *C. populi* for 2 weeks.

Supplemental Figure S3. Feeding damage to the top leaves of poplars during *C. populi* feeding and rank scale for the scores to determine leaf damage.

Supplemental Figure S4. Pathway analysis of flavonoid biosynthesis.

Supplemental Figure S5. Pathway analysis of phenylacetaldoxime biosynthesis.

Supplemental Figure S6. Statistical analysis of the GC-MS data for VOCs.

Supplemental Figure S7. Overview of the mass difference analysis workflow, which aims to map the transcriptomic data on their respective MDBs.

Supplemental Figure S8. Compositional space of discriminant molecular formulas.

Supplemental Table S1. Data file for genes with significantly increased or decreased transcript abundance in poplar leaves in response to EMF inoculation with *L. bicolor* or attack by *C. populi* beetles, results of GO Slim analysis, count data of selected stress genes, and validation of RNAseq.

Supplemental Table S2. Characteristics of the VOCs sampled from *P.* × *canescens* trees.

Supplemental Table S3. VOCs emitted by poplar leaves in response to mycorrhizal inoculation and leaf beetle feeding.

Supplemental Table S4. Data files for annotated molecular formulas of the FT-ICR-MS and negative and positive LC-MS measurements.

Supplemental Table S5. Data file for mass difference enrichment analysis results.

Supplemental Methodology S1. How does mass difference enrichment analysis enhance metabolomics?

ACKNOWLEDGMENTS

We thank C. Kettner, M. Franke-Klein, T. Klein, G. Langer-Kettner, and M. Smiatacz (University of Göttingen) for maintenance of plants and fungi in culture and under free air conditions, for help with the harvest, and for excellent technical assistance. We thank Sara Forcisi and Kirill Smirnov (Helmholtz Zentrum München) for the development of the standard operation procedure for UPLC-qToF-MS analysis and Dr. D. Euring (University of Göttingen) for providing the primers for reverse transcription-quantitative PCR.

Received January 2, 2018; accepted January 18, 2018; published February 8, 2018.

LITERATURE CITED

Allwright MR, Payne A, Emiliani G, Milner S, Viger M, Rouse F, Keurentjes JJB, Bérard A, Wildhagen H, Faivre-Rampant P, et al (2016) Biomass traits and candidate genes for bioenergy revealed through association genetics in coppiced European *Populus nigra* (L.). Biotechnol Biofuels **9:** 195

Arimura G, Huber DPW, Bohlmann J (2004) Forest tent caterpillars (*Malacosoma disstria*) induce local and systemic diurnal emissions of terpenoid volatiles in hybrid poplar (*Populus trichocarpa* × *deltoides*): cDNA cloning, functional characterization, and patterns of gene expression of (−)-germacrene D synthase, PtdTPS1. Plant J **37:** 603–616

Arimura G, Kost C, Boland W (2005) Herbivore-induced, indirect plant defences. Biochim Biophys Acta **1734:** 91–111

Arimura G, Matsui K, Takabayashi J (2009) Chemical and molecular ecology of herbivore-induced plant volatiles: proximate factors and their ultimate functions. Plant Cell Physiol **50:** 911–923

Bates D, Maechler M, Bolker B, Walker S (2015) Fitting linear mixed-effects models using lme4. J Stat Softw **67:** 1–48

Bauer S, Grossmann S, Vingron M, Robinson PN (2008) Ontologizer 2.0: a multifunctional tool for GO term enrichment analysis and data exploration. Bioinformatics **24:** 1650–1651

Baum C, Toljander YK, Eckhardt KU, Weih M (2009) The significance of host-fungus combinations in ectomycorrhizal symbioses for the chemical quality of willow foliage. Plant Soil **323:** 213–224

Behnke K, Kaiser A, Zimmer I, Brüggemann N, Janz D, Polle A, Hampp R, Hänsch R, Popko J, Schmitt-Kopplin P, et al (2010) RNAi-mediated suppression of isoprene emission in poplar impacts phenolic metabolism under high temperature and high light intensities: a transcriptomic and metabolomic analysis. Plant Mol Biol **74:** 61–75

Benjamini Y, Hochberg Y (1995) Controlling the false discovery rate: a practical and powerful approach to multiple testing. J R Stat Soc **57:** 289–300

Bidartondo MI, Ek H, Wallander H, Söderström B (2001) Do nutrient additions alter carbon sink strength of ectomycorrhizal fungi? New Phytol **151:** 543–550

Boeckler GA, Gershenzon J, Unsicker SB (2011) Phenolic glycosides of the Salicaceae and their role as anti-herbivore defenses. Phytochemistry **72:** 1497–1509

Boeckler GA, Towns M, Unsicker SB, Mellway RD, Yip L, Hilke I, Gershenzon J, Constabel CP (2014) Transgenic upregulation of the condensed tannin pathway in poplar leads to a dramatic shift in leaf palatability for two tree-feeding Lepidoptera. J Chem Ecol **40:** 150–158

Brilli F, Ciccioli P, Frattoni M, Prestininzi M, Spanedda AF, Loreto F (2009) Constitutive and herbivore-induced monoterpenes emitted by Populus × euroamericana leaves are key volatiles that orient Chrysomela populi beetles. Plant Cell Environ **32:** 542–552

Chang S, Puryear J, Cairney J (1993) A simple and efficient method for isolating RNA from pine trees. Plant Mol Biol Rep **11:** 113–116

Clarke HRG, Lawrence SD, Flaskerud J, Korhnak TE, Gordon MP, Davis JM (1998) Chitinase accumulates systemically in wounded poplar trees. Physiol Plant **103:** 154–161

Collinge DB, Kragh KM, Mikkelsen JD, Nielsen KK, Rasmussen U, Vad K (1993) Plant chitinases. Plant J **3:** 31–40

Colpaert JV, Van Assche JA, Luijtens K (1992) The growth of the extramatrical mycelium of ectomycorrhizal fungi and the growth response of *Pinus sylvestris* L. New Phytol **120:** 127–135

Coviella CE, Stipanovic RD, Trumble JT (2002) Plant allocation to defensive compounds: interactions between elevated CO_2 and nitrogen in transgenic cotton plants. J Exp Bot **53:** 323–331

Danielsen L, Lohaus G, Sirrenberg A, Karlovsky P, Bastien C, Pilate G, Polle A (2013) Ectomycorrhizal colonization and diversity in relation to tree biomass and nutrition in a plantation of transgenic poplars with modified lignin biosynthesis. PLoS ONE **8:** e59207

Danielsen L, Polle A (2014) Poplar nutrition under drought as affected by ectomycorrhizal colonization. Environ Exp Bot **108:** 89–98

Delker C, Stenzel I, Hause B, Miersch O, Feussner I, Wasternack C (2006) Jasmonate biosynthesis in *Arabidopsis thaliana*: enzymes, products, regulation. Plant Biol (Stuttg) **8:** 297–306

De Moraes CM, Lewis WJ, Pare PW, Alborn HT, Tumlinson JH (1998) Herbivore-infested plants selectively attract parasitoids. Nature **393:** 570–573

Díaz-Pines E, Molina-Herrera S, Dannenmann M, Braun J, Haas E, Willibald G, Arias-Navarro C, Grote R, Wolf B, Saiz G, et al (2016) Nitrate leaching and nitrous oxide emissions diminish with time in a hybrid poplar short-rotation coppice in southern Germany. Glob Change Biol Bioenergy **9:** 613–626

Ditengou FA, Müller A, Rosenkranz M, Felten J, Lasok H, van Doorn MM, Legué V, Palme K, Schnitzler JP, Polle A (2015) Volatile signalling by sesquiterpenes from ectomycorrhizal fungi reprogrammes root architecture. Nat Commun **6:** 6279

Dučić T, Parladé J, Polle A (2008) The influence of the ectomycorrhizal fungus *Rhizopogon subareolatus* on growth and nutrient element localisation in two varieties of Douglas fir (*Pseudotsuga menziesii* var. *menziesii* and var. *glauca*) in response to manganese stress. Mycorrhiza **18:** 227–239

Edwards R, Dixon DP, Walbot V (2000) Plant glutathione S-transferases: enzymes with multiple functions in sickness and in health. Trends Plant Sci **5:** 193–198

Ejigu BA, Valkenborg D, Baggerman G, Vanaerschot M, Witters E, Dujardin JC, Burzykowski T, Berg M (2013) Evaluation of normalization methods to pave the way towards large-scale LC-MS-based metabolomics profiling experiments. OMICS **17:** 473–485

Ek H (1997) The influence of nitrogen fertilization on the carbon economy of *Paxillus involutus* in ectomycorrhizal association *with Betula pendula*. New Phytol **135:** 133–142

Finlay RD (2008) Ecological aspects of mycorrhizal symbiosis: with special emphasis on the functional diversity of interactions involving the extraradical mycelium. J Exp Bot **59:** 1115–1126

Fontana A, Reichelt M, Hempel S, Gershenzon J, Unsicker SB (2009) The effects of arbuscular mycorrhizal fungi on direct and indirect defense metabolites of *Plantago lanceolata* L. J Chem Ecol **35:** 833–843

Forcisi S, Moritz F, Lucio M, Lehmann R, Stefan N, Schmitt-Kopplin P (2015) Solutions for low and high accuracy mass spectrometric data matching: a data-driven annotation strategy in nontargeted metabolomics. Anal Chem **87:** 8917–8924

Gange AC, Gane DR, Chen Y, Gong M (2005) Dual colonization of *Eucalyptus urophylla* ST Blake by arbuscular and ectomycorrhizal fungi affects levels of insect herbivore attack. Agric For Entomol **7:** 253–263

Gange AC, West HM (1994) Interactions between arbuscular mycorrhizal fungi and foliar-feeding insects in *Plantago lanceolata* L. New Phytol **128:** 79–87

Gehring C, Bennett A (2009) Mycorrhizal fungal-plant-insect interactions: the importance of a community approach. Environ Entomol **38:** 93–102

Georgi R, Helbig C, Schubert M (2012) The red poplar leaf beetle in short rotation coppice. AFZ Wald **67:** 11–13

Goossens J, Fernández-Calvo P, Schweizer F, Goossens A (2016) Jasmonates: signal transduction components and their roles in environmental stress responses. Plant Mol Biol **91:** 673–689

Halldórsson G, Sverrisson H, Eyjólfsdóttir GG, Oddsdóttir ES (2000) Ectomycorrhizae reduce damage to Russian larch by Otiorhyncus larvae. Scand J For Res **15:** 354–358

Harding SA, Jarvie MM, Lindroth RL, Tsai CJ (2009) A comparative analysis of phenylpropanoid metabolism, N utilization, and carbon partitioning in fast- and slow-growing *Populus* hybrid clones. J Exp Bot **60:** 3443–3452

Harrell MO, Benjamin DM, Berbee JG, Burkot TR (1981) Evaluation of adult cottonwood leaf beetle, *Chrysomela scripta* (Coleoptea, Chrysomelidae) feeding preference for hybrid poplars. Great Lakes Entomol **14:** 181–184

Hartley SE, Gange AC (2009) Impacts of plant symbiotic fungi on insect herbivores: mutualism in a multitrophic context. Annu Rev Entomol **54:** 323–342

Hatanaka A (1993) The biogeneration of green odour by green leaves. Phytochemistry **34:** 1201–1218

Hothorn T, Bretz F, Westfall P (2008) Simultaneous inference in general parametric models. Biom J **50:** 346–363

Ikonen A (2002) Preferences of six leaf beetle species among qualitatively different leaf age classes of three Salicaceous host species. Chem Ecol **12:** 23–28

Irmisch S, McCormick AC, Boeckler GA, Schmidt A, Reichelt M, Schneider B, Block K, Schnitzler JP, Gershenzon J, Unsicker SB, et al (2013) Two herbivore-induced cytochrome P450 enzymes CYP79D6 and CYP79D7 catalyze the formation of volatile aldoximes involved in poplar defense. Plant Cell **25:** 4737–4754

Irmisch S, McCormick AC, Günther J, Schmidt A, Boeckler GA, Gershenzon J, Unsicker SB, Köllner TG (2014) Herbivore-induced poplar cytochrome P450 enzymes of the CYP71 family convert aldoximes to nitriles which repel a generalist caterpillar. Plant J **80:** 1095–1107

Jung HW, Tschaplinski TJ, Wang L, Glazebrook J, Greenberg JT (2009) Priming in systemic plant immunity. Science **324:** 89–91

Jung SC, Martinez-Medina A, Lopez-Raez JA, Pozo MJ (2012) Mycorrhiza-induced resistance and priming of plant defenses. J Chem Ecol **38:** 651–664

Kaling M, Kanawati B, Ghirardo A, Albert A, Winkler JB, Heller W, Barta C, Loreto F, Schmitt-Kopplin P, Schnitzler JP (2015) UV-B mediated metabolic rearrangements in poplar revealed by non-targeted metabolomics. Plant Cell Environ **38:** 892–904

Kavka M, Polle A (2016) Phosphate uptake kinetics and tissue-specific transporter expression profiles in poplar (*Populus* × *canescens*) at different phosphorus availabilities. BMC Plant Biol **16:** 206

Keski-Saari S, Julkunen-Tiitto R (2003) Resource allocation in different parts of juvenile mountain birch plants: effect of nitrogen supply on seedling phenolics and growth. Physiol Plant **118:** 114–126

Kikuta Y, Ueda H, Nakayama K, Katsuda Y, Ozawa R, Takabayashi J, Hatanaka A, Matsuda K (2011) Specific regulation of pyrethrin biosynthesis in *Chrysanthemum cinerariaefolium* by a blend of volatiles emitted from artificially damaged conspecific plants. Plant Cell Physiol **52:** 588–596

Koricheva J, Gange AC, Jones T (2009) Effects of mycorrhizal fungi on insect herbivores: a meta-analysis. Ecology **90:** 2088–2097

Langenfeld-Heyser R, Gao J, Ducic T, Tachd P, Lu CF, Fritz E, Gafur A, Polle A (2007) *Paxillus involutus* mycorrhiza attenuate NaCl-stress responses in the salt-sensitive hybrid poplar *Populus* × *canescens*. Mycorrhiza **17:** 121–131

Larose G, Chênevert R, Moutoglis P, Gagné S, Piché Y, Vierheilig H (2002) Flavonoid levels in roots of *Medicago sativa* are modulated by the developmental stage of the symbiosis and the root colonizing arbuscular mycorrhizal fungus. J Plant Physiol **159:** 1329–1339

Lawrence SD, Novak NG (2006) Expression of poplar chitinase in tomato leads to inhibition of development in Colorado potato beetle. Biotechnol Lett **28:** 593–599

Lea US, Leydecker MT, Quilleré I, Meyer C, Lillo C (2006) Posttranslational regulation of nitrate reductase strongly affects the levels of free amino acids and nitrate, whereas transcriptional regulation has only minor influence. Plant Physiol **140:** 1085–1094

Li FR, Dudley TL, Chen BM, Chang XY, Liang LY, Peng SL (2016) Responses of tree and insect herbivores to elevated nitrogen inputs: a meta-analysis. Acta Oecolog **77:** 160–167

Lindroth RL, St Clair SB (2013) Adaptations of trembling aspen (*P. tremuloides* Michx.) for defense against herbivores. For Ecol Manage **299:** 14–21

Lucio M, Fekete A, Frommberger M, Schmitt-Kopplin P (2011) Metabolomics: high-resolution tools offer to follow bacterial growth on a molecular level. *In* FJ de Bruijn, ed, Handbook of Molecular Microbial Ecology I: Metagenomics and Complementary Approaches. John Wiley & Sons, Hoboken, NJ, doi/10.1002/9781118010518.ch72

Luo ZB, Janz D, Jiang X, Göbel C, Wildhagen H, Tan Y, Rennenberg H, Feussner I, Polle A (2009) Upgrading root physiology for stress tolerance by ectomycorrhizas: insights from metabolite and transcriptional profiling into reprogramming for stress anticipation. Plant Physiol **151:** 1902–1917

Luo ZB, Li K, Gai Y, Göbel C, Wildhagen H, Jiang X, Feußner I, Rennenberg H, Polle A (2011) The ectomycorrhizal fungus (*Paxillus involutus*) modulates leaf physiology of poplar towards improved salt tolerance. Environ Exp Bot **72:** 304–311

Madritch MD, Lindroth RL (2015) Condensed tannins increase nitrogen recovery by trees following insect defoliation. New Phytol **208:** 410–420

Major IT, Constabel CP (2006) Molecular analysis of poplar defense against herbivory: comparison of wound- and insect elicitor-induced gene expression. New Phytol **172:** 617–635

Manninen AM, Holopainen T, Holopainen JK (1998) Susceptibility of ectomycorrhizal and non-mycorrhizal Scots pine (*Pinus sylvestris*) seedlings to a generalist insect herbivore, *Lygus rugulipennis*, at two nitrogen availability levels. New Phytol **140:** 55–63

Matsuda K (2012) Pyrethrin biosynthesis and its regulation *in Chrysanthemum cinerariaefolium*. Top Curr Chem **314:** 73–81

Matsuda K, Matsuo H (1985) A flavonoid, luteolin-7-glucoside, as well as salicin and populin, stimulating the feeding of leaf beetles attacking salicaceous plants. Appl Entomol Zool (Jpn) **20:** 305–313

Matsui K (2006) Green leaf volatiles: hydroperoxide lyase pathway of oxylipin metabolism. Curr Opin Plant Biol **9:** 274–280

McCormick AC, Irmisch S, Reinecke A, Boeckler GA, Veit D, Reichelt M, Hansson BS, Gershenzon J, Köllner TG, Unsicker SB (2014) Herbivore-induced volatile emission in black poplar: regulation and role in attracting herbivore enemies. Plant Cell Environ **37:** 1909–1923

McCormick AC, Unsicker SB, Gershenzon J (2012) The specificity of herbivore-induced plant volatiles in attracting herbivore enemies. Trends Plant Sci **17:** 303–310

Moritz F, Janicka M, Zygler A, Forcisi S, Kot-Wasik A, Kot J, Gebefügi I, Namiesnik J, Schmitt-Kopplin P (2015) The compositional space of exhaled breath condensate and its link to the human breath volatilome. J Breath Res **9:** 027105

Moritz F, Kaling M, Schnitzler JP, Schmitt-Kopplin P (2017) Characterization of poplar metabotypes via mass difference enrichment analysis. Plant Cell Environ **40:** 1057–1073

Müller A, Kaling M, Faubert P, Gort G, Smid HM, Van Loon JJ, Dicke M, Kanawati B, Schmitt-Kopplin P, Polle A, et al (2015) Isoprene emission by poplar is not important for the feeding behaviour of poplar leaf beetles. BMC Plant Biol **15:** 165

Müller A, Volmer K, Mishra-Knyrim M, Polle A (2013) Growing poplars for research with and without mycorrhizas. Front Plant Sci **4:** 332

Muzika RM (1993) Terpenes and phenolics in response to nitrogen fertilization: a test of the carbon/nutrient balance hypothesis. Chemoecology **4:** 3–7

Nehls U, Göhringer F, Wittulsky S, Dietz S (2010) Fungal carbohydrate support in the ectomycorrhizal symbiosis: a review. Plant Biol (Stuttg) **12:** 292–301

Nerg AM, Kasurinen A, Holopainen T, Julkunen-Tiitto R, Neuvonen S, Holopainen JK (2008) The significance of ectomycorrhizas in chemical quality of silver birch foliage and above-ground insect herbivore performance. J Chem Ecol **34:** 1322–1330

Oddsdottir ES, Eilenberg J, Sen R, Harding S, Halldorsson G (2010) Early reduction of *Otiorhynchus* spp. larval root herbivory on *Betula pubescens* by beneficial soil fungi. Appl Soil Ecol **45:** 168–174

Pfabel C, Eckhardt KU, Baum C, Struck C, Frey P, Weih M (2012) Impact of ectomycorrhizal colonization and rust infection on the secondary metabolism of poplar (*Populus trichocarpa* × *deltoides*). Tree Physiol **32:** 1357–1364

Philippe RN, Bohlmann J (2007) Poplar defense against insect herbivores. Can J Bot **85:** 1111–1126

Pieterse CMJ, Zamioudis C, Berendsen RL, Weller DM, Van Wees SCM, Bakker PAHM (2014) Induced systemic resistance by beneficial microbes. Annu Rev Phytopathol **52:** 347–375

Pineda A, Dicke M, Pieterse CMJ, Pozo MJ (2013) Beneficial microbes in a changing environment: are they always helping plants to deal with insects? Funct Ecol **27:** 574–586

Polle A, Chakrabarti K, Schürmann W, Renneberg H (1990) Composition and properties of hydrogen peroxide decomposing systems in extracellular and total extracts from needles of Norway spruce (*Picea abies* L., Karst.). Plant Physiol **94:** 312–319

Polle A, Douglas C (2010) The molecular physiology of poplars: paving the way for knowledge-based biomass production. Plant Biol (Stuttg) **12:** 239–241

R Core Team (2015) R: A Language and Environment for Statistical Computing. R Foundation for Statistical Computing, Vienna

Rieske LK, Rhoades CC, Miller SP (2003) Foliar chemistry and gypsy moth, *Lymantria dispar* (L.), herbivory on pure American chestnut, *Castanea dentata* (Fam: Fagaceae), and a disease-resistant hybrid. Environ Entomol **32:** 359–365

Robinson MD, McCarthy DJ, Smyth GK (2010) edgeR: a Bioconductor package for differential expression analysis of digital gene expression data. Bioinformatics **26:** 139–140

Rowell-Rahier M, Pasteels JM (1986) Economics of chemical defense in Chrysomelinae. J Chem Ecol **12:** 1189–1203

Ruan J, Haerdter R, Gerendás J (2010) Impact of nitrogen supply on carbon/nitrogen allocation: a case study on amino acids and catechins in green tea [*Camellia sinensis* (L.) O. Kuntze] plants. Plant Biol (Stuttg) **12:** 724–734

Rubert-Nason KF, Couture JJ, Major IT, Constabel CP, Lindroth RL (2015) Influence of genotype, environment, and gypsy moth herbivory on local and systemic chemical defenses in trembling aspen (*Populus tremuloides*). J Chem Ecol **41:** 651–661

Rygiewicz PT, Anderson CP (1994) Mycorrhizae alter quality and quantity of carbon allocated below ground. Nature **369:** 58–60

Salvioli A, Bonfante P (2013) Systems biology and "omics" tools: a cooperation for next-generation mycorrhizal studies. Plant Sci **203-204:** 107–114

Schopfer P (1989) Experimentelle Pflanzenphysiologie, Band 2: Einführung in die Anwendungen. Springer Verlag, Heidelberg, Germany, pp 349–353

Schweiger R, Baier MC, Persicke M, Müller C (2014) High specificity in plant leaf metabolic responses to arbuscular mycorrhiza. Nat Commun **5:** 3886

Su Y, Xu L, Wang S, Wang Z, Yang Y, Chen Y, Que Y (2015) Identification, phylogeny, and transcript of chitinase family genes in sugarcane. Sci Rep **5:** 10708

Suhre K, Schmitt-Kopplin P (2008) MassTRIX: mass translator into pathways. Nucleic Acids Res **36:** W481–W484

Takahashi M, Terada Y, Nakai I, Nakanishi H, Yoshimura E, Mori S, Nishizawa NK (2003) Role of nicotianamine in the intracellular delivery of metals and plant reproductive development. Plant Cell **15:** 1263–1280

Tholl D, Boland W, Hansel A, Loreto F, Röse USR, Schnitzler JP (2006) Practical approaches to plant volatile analysis. Plant J **45:** 540–560

Tsai CJ, Harding SA, Tschaplinski TJ, Lindroth RL, Yuan Y (2006) Genome-wide analysis of the structural genes regulating defense phenylpropanoid metabolism in *Populus*. New Phytol **172:** 47–62

Tsai CJ, Ranjan P, DiFazio SP, Tuskan GA, Johnson V (2011) Poplar genome microarrays. *In* CP Joshi, SP DiFazio, C Kole, eds, Genetics, Genomics and Breeding of Poplars. Science Publishers, Boca Raton, FL, pp 112–127

Tziotis D, Hertkorn N, Schmitt-Kopplin P (2011) Kendrick-analogous network visualisation of ion cyclotron resonance Fourier transform mass spectra: improved options for the assignment of elemental compositions and the classification of organic molecular complexity. Eur J Mass Spectrom (Chichester) **17:** 415–421

Urban J (2006) Occurrence, bionomics and harmfulness of *Chrysomela populi* L. (Coleoptera, Chrysomelidae). J Sci **52:** 255–284

van Dam NM, Qiu BL, Hordijk CA, Vet LEM, Jansen JJ (2010) Identification of biologically relevant compounds in aboveground and belowground induced volatile blends. J Chem Ecol **36:** 1006–1016

van den Dool H, Kratz PDA (1962) Generalization of the retention index system including linear temperature programmed gas-liquid partition chromatography. J Chromatogr **11:** 463–471

von Wiren N, Klair S, Bansal S, Briat JF, Khodr H, Shioiri T, Leigh RA, Hider RC, (1999) Nicotianamine chelates both FeIII and FeII: implications for metal transport in plants. Plant Physiol **119:** 1107–1114

Weikl, F, Ghirardo A, Schnitzler JP, Pritsch K (2016) Sesquiterpene emissions from Alternaria alternata: effects of age, nutrient availability, and co-cultivation with Fusarium oxysporum. Sci Rep **6:** srep22152

Wittek F, Hoffmann T, Kanawati B, Bichlmeier M, Knappe C, Wenig M, Schmitt-Kopplin P, Parker JE, Schwab W, Vlot AC (2014) *Arabidopsis* ENHANCED DISEASE SUSCEPTIBILITY1 promotes systemic acquired resistance via azelaic acid and its precursor 9-oxo nonanoic acid. J Exp Bot **65:** 5919–5931

Yang KY, Moon YH, Choi KH, Kim YH, Eun MY, Guh JO, Kim KC, Cho BH (1997) Structure and expression of the AWI 31 gene specifically induced by wounding in *Arabidopsis thaliana*. Mol Cells **7:** 131–135

Zeilinger S, Gupta VK, Dahms TES, Silva RN, Singh HB, Upadhyay RS, Gomes EV, Tsui CKM, Nayak SC (2016) Friends or foes? Emerging insights from fungal interactions with plants. FEMS Microbiol Rev **40:** 182–207

Zheng L, Cheng Z, Ai C, Jiang X, Bei X, Zheng Y, Glahn RP, Welch RM, Miller DD, Lei XG, et al (2010) Nicotianamine, a novel enhancer of rice iron bioavailability to humans. PLoS One **5:** e10190